1 **piRNA processing by a trimeric Schlafen-domain nuclease**

2

3 Nadezda Podvalnaya[1,2,*], Alfred W. Bronkhorst[1,*], Raffael Lichtenberger[3], Svenja Hellmann[1],

4 Emily Nischwitz[2,4], Torben Falk[3], Emil Karaulanov[5], Falk Butter[4], Sebastian Falk[3,#], René F.

5 Ketting[1,6,#]

6

7 [1] Biology of Non-coding RNA group, Institute of Molecular Biology, Ackermannweg 4, 55128

8 Mainz, Germany

9 [2] International PhD Programme on Gene Regulation, Epigenetics & Genome Stability, Mainz,

10 Germany

11 [3] Department of Structural and Computational Biology, Max Perutz Labs, University of Vienna,

12 1030 Vienna, Austria

13 [4] Quantitative Proteomics group, Institute of Molecular Biology, Ackermannweg 4, 55128

14 Mainz, Germany

15 [5] Bioinformatics Core Facility, Institute of Molecular Biology, Ackermannweg 4, 55128 Mainz,

16 Germany

17 [6] Institute of Developmental Biology and Neurobiology, Johannes Gutenberg University,

18 55099 Mainz, Germany

19

20

21 *: Equally contributed

22 #: Shared correspondence: sebastian.falk@univie.ac.at; r.ketting@imb-mainz.de

23

1 **Abstract**

2 Transposable elements are genomic parasites that expand within and spread between

3 genomes[1]. Piwi proteins control transposon activity, notably in the germline[2,3]. These proteins

4 recognize their targets through small RNA co-factors named piRNAs, making piRNA biogenesis

5 a key specificity-determining step in this crucial genome immunity system. While the

6 processing of piRNA precursors is an essential step in this process, many molecular details of

7 this process remain unknown. We identify a novel endoribonuclease, PUCH, that initiates

8 piRNA processing in the nematode *Caenorhabditis elegans*. Genetic and biochemical studies

9 show that PUCH, a trimer of Schlafen-like-domain proteins (SLFL proteins), executes 5'-end

10 piRNA precursor cleavage. PUCH-mediated processing strictly requires an m7G-Cap and a

11 uracil at position three. We also demonstrate how PUCH interacts with PETISCO, a complex

12 that binds piRNA precursors[4], and that this interaction enhances piRNA production *in vivo*.

13 The identification of PUCH completes the repertoire of *C. elegans* piRNA biogenesis factors

14 and uncovers a novel type of RNA endonuclease formed by three SLFL proteins. Mammalian

15 Schlafen (Slfn) genes have been associated with immunity responses[5], exposing a thus far

16 unknown molecular link between immune responses in mammals and deeply conserved RNA-

17 based mechanisms that control transposable elements.

18

**Introduction**

Transposable elements (TEs) are segments of DNA that can independently multiply and move within, and sometimes between genomes[1]. Being found in virtually all genomes analyzed to date, transposons are clearly highly successful, and hence their control, especially in the germ cells, is an essential process. Interestingly, TEs can mutate to avoid defense systems, and in turn, defense systems can adapt to such changes, resulting in a molecular arms race, leading to rapid diversification between species[6]. Small RNA-driven gene regulatory pathways represent one of the mechanisms through which transposable elements are controlled[2,3]. In the germ cells of animals, Argonaute proteins of the Piwi clade interact with so-called piRNAs to control transposons, but also host genes[7]. This regulatory process is essential for germ cell function and fertility. Consistent with a role in TE defense, piRNA pathways are characterized by many species-specific factors, even though piRNA pathways also share deeply conserved concepts[2,3].

The production of piRNAs is essential, as the piRNAs portfolio defines the target range and specificity of the Piwi-piRNA pathway. Mature piRNAs are generated from longer, single-stranded piRNA precursor molecules[2,3,8]. In all systems analyzed, this process is started by a nucleolytic cleavage, which defines the 5'-end of a new piRNA. In *Drosophila* and mouse, Piwi mediated cleavage (slicer activity) can generate such a 5'-end, which then is bound by a new Piwi protein. The net effect of this process is the amplification of piRNAs through Piwi cleavage. Moreover, the Piwi protein that binds to the newly generated 5'-end recruits an endonuclease named Zucchini (Zuc), or PhospholipaseD6 (PLD6)[9–12]. Zuc induces an additional break, and thus an additional 5'-end, downstream of the bound Piwi protein, which can again be bound by a Piwi protein [13,14]. This process not only amplifies but also diversifies piRNA populations. The current model suggests that after 5'-end processing the 3'-end is formed following binding to a Piwi protein. This step involves trimming by 3'-5' exoribonuclease activity and methylation of the 2' OH at the 3'-end. In *C. elegans* this is done by PARN-1[15] and HENN-1 respectively[16–18].

Interestingly, not all animals rely on Zuc/PLD6 and/or Piwi for piRNA biogenesis. Notably, *C. elegans* lacks a Zuc homolog. Furthermore, the slicer activity of the *C. elegans* Piwi homolog

1    (PRG-1[19–21]) is not needed for piRNA production[22], making it a great unknown how piRNA 5'-

2    ends are generated. In this nematode, piRNA precursors are transcribed from short genes,

3    each encoding one piRNA, which in *C. elegans* is also named 21U RNA[23]. The precursors are

4    roughly 27-29 nucleotides long and carry a 5'-Cap (**Fig. 1a**)[24]. Since these precursors are not

5    trans-spliced, this Cap is most likely an m7-G Cap. We note that in contrast to many other

6    animals, including mammals, *C. elegans* does not place m7-G Caps on canonical mRNAs, but

7    2,2,7-trimethyl-G Caps (TMG-Cap) through a process of 5'-end trans-splicing[25]. It is thus

8    possible that the m7-G Cap can be a feature that helps distinguish between piRNA precursors

9    and mRNAs. Following transcription by specialized machinery[26,27], the precursors are bound

10   by PETISCO, a cytoplasmic protein complex consisting of PID-3, ERH-2, TOFU-6 and IFE-3[4,28–

11   30]. While PETISCO has been implicated in precursor stabilization and is required for piRNA

12   production, it contains no nucleases. Hence, the nuclease that mediates 5' precursor

13   processing and how it interact with PETISCO remains unidentified.

14

15   **TOFU-2 interacts with TOFU-1 and is a potential nuclease**

16   A genome-wide RNAi screen identified the proteins TOFU-1 and TOFU-2 as factors necessary

17   for piRNA accumulation[31]. Loss of these factors also triggered piRNA precursor accumulation,

18   suggesting they may play a role in piRNA 5'-end processing. However, domain annotations at

19   that time did not reveal potential nuclease domains. Using structure-based homology

20   searches (HHPRED)[32] and AlphaFold2 (AF2)[33], we detected homology between TOFU-1 and

21   TOFU-2, and the rat ribonuclease Schlafen13 (SLFN13)[34], but also human Schlafen5[35] and

22   Schlafen12[36]. This identified the presence of a potential SLFN-fold in both TOFU-1 and TOFU-

23   2 (**Fig. 1b,c**). Interestingly, whereas in mammalian Schlafen proteins two SLFN-folds come

24   together to form the nuclease domain[34–36], in TOFU-1 and TOFU-2 only one SLFN-fold could

25   be identified. Hence, we hypothesized that TOFU-1 and TOFU-2 may interact to form a

26   functional nuclease. To test this hypothesis, we tagged endogenous TOFU-2 with a Human

27   influenza hemagglutinin (HA)-tag and used immuno-precipitation (IP) followed by

28   quantitative mass spectrometry (MS) to identify TOFU-2 interacting proteins. Indeed, TOFU-

29   1 was found to interact with TOFU-2 (**Fig.1d; Table S1**). Potential catalytic residues were

30   identified within TOFU-2, but not TOFU-1 (**Fig.1c, Suppl. Fig.1a**). Thus, we engineered a *C.*

31   *elegans tofu-2* mutant in which we changed one of the potential catalytic residues (glutamic

1  acid 216) to alanine (E216A). This mutation neither affects TOFU-2 abundance nor interaction

2  with TOFU-1, as judged by Western blot analysis and IP-MS analysis (**Suppl. Fig.1c,d; Table**

3  **S2**). Next, we tested piRNA silencing activity in this mutant, using a so-called piRNA-sensor (a

4  germline-expressed transgene that is silenced through piRNA activity[22]) (**Fig.1e**). This revealed

5  that *tofu-2(e216a)* mutants de-silence the piRNA-sensor to a similar extent as *prg-1* mutants

6  (**Fig.1f**). Sequencing of piRNAs and piRNA precursors showed that *tofu-2(e216a)* mutants lost

7  almost all mature piRNAs, while accumulating precursors (**Fig.1g, h, Suppl. Fig.1e**), suggesting

8  that a TOFU-1:TOFU-2 complex could be the nuclease that processes piRNA precursors.

9

10  **TOFU-1 and TOFU-2 interact with SLFL-3 or SLFL-4 to form a trimeric complex**

11  Next, we heterologously expressed TOFU-1 and TOFU-2 in BmN4 cells, a silk-moth derived cell

12  culture system that expressed these proteins well, and found that TOFU-1 and TOFU-2 co-

13  immunoprecipitate (coIP) each other (**Fig.2a, lane 4**). However, incubating the coIPs with a

14  synthetic piRNA precursor did not result in precursor cleavage (see next section), suggesting

15  that our experimental conditions might lack an essential cofactor.

16

17  The TOFU-2 IP-MS experiments, in addition to TOFU-1, also identified the proteins C35E7.8

18  and F36H12.2 (**Fig.1d, Suppl. Fig.1a,b**). These two proteins are 90% identical at the amino-

19  acid level (**Suppl. Fig.2a**) and hence may function redundantly. Analysis with AF2[33,37] revealed

20  that these two proteins also contain a single potential SLFN-like fold (**Suppl. Fig.2b**).

21  Therefore, we propose the name "SLFN-like", or SLFL, for this group of proteins that only

22  contain a single SLFN-fold, with TOFU-1, TOFU-2, C35E7.8 and F36H12.2 corresponding to

23  SLFL-1, SLFL-2, SLFL-3 and SLFL-4 respectively. Interestingly, SLFL-3 was identified in the same

24  study that identified TOFU-1 and TOFU-2, but its RNAi-mediated knock-down triggered a

25  relatively weak reduction in piRNA levels and was not investigated further[31]. We generated a

26  *slfl-3* deletion mutant (**Suppl. Fig.2c**) and found that this allele triggers reduced piRNA activity,

27  as evidenced by a mild activation of the piRNA sensor (**Suppl. Fig.2d**). In addition to the SLFN-

28  like fold, SLFL-3 and SLFL-4 also contain a predicted transmembrane (TM) helix (**Suppl.**

29  **Fig.2a,e**), a feature that is also present in mammalian and *Drosophila* Zuc[38,39]. By transfecting

30  BmN4 cells with TOFU-1, eGFP-TOFU-2 and mCherry-SLFL-3 carrying or lacking the TM, we

31  could show that the TM of SLFL-3 localizes to mitochondria (**Fig.2b**). Interestingly, TOFU-2

32  colocalizes with SLFL-3 suggesting they form a complex.

1 We used AF2[33,40] to predict how these four SLFL proteins may interact with each other. This

2 revealed that a trimeric combination of TOFU-1, TOFU-2 and either SLFL-3 or SLFL-4 yielded

3 the best predictions, in which the three SLFN domains were found to interact with each other

4 (**Fig. 2c**, **Suppl. Fig.3**). Further fine-tuning of the procedure produced a high-confidence model

5 of TOFU-1, TOFU-2 and SLFL-3 (**Fig. 2c**, **Suppl. Fig.4**) suggesting that the active nuclease may

6 be a trimeric complex. This prompted us to co-express TOFU-1, TOFU-2 and either SLFL-3 or

7 SLFL-4 in BmN4 cells and to test their interaction through coIP experiments. Indeed, these

8 experiments support the idea of a trimer. For instance, TOFU-2 is expressed at higher levels

9 if co-expressed with TOFU-1 and SLFL-3 and TOFU-2 only coIPs with SLFL-3 in the presence of

10 TOFU-1 (**Fig.2a**).

11

12 We also assessed the interactions between TOFU-1, TOFU-2 and SLFL-3 through heterologous

13 expression and coIP experiments in *E. coli* (**Suppl. Fig.5a**). While the TOFU-2 SPRY domain did

14 not display strong interactions (**Suppl. Fig.5b**), TOFU-1 and SLFL-3 interacted with their SLFN-

15 domain directly with the TOFU-2 SLFN domain (**Suppl. Fig.5c-d**), and a complex containing all

16 three proteins could be readily identified (**Suppl. Fig.5e**). These findings are in line with the

17 AF2 model (**Suppl. Fig.4**) and the coIPs from BmN4 cells (**Fig.2a**).

18

19 **TOFU-1:TOFU-2:SLFN-3/4 complexes process piRNA precursors**

20 Next, we tested coIPs from BmN4 cells in which we co-expressed different combinations of

21 TOFU-1, TOFU-2, SLFL-3 and SLFL-4 for piRNA processing activity. As substrate, we used a

22 synthetic piRNA precursor oligonucleotide carrying an m7-G cap, which was radioactively

23 labelled at its 3'-end with $^{32}$P for detection (**Fig.3a**). Processing activity was analyzed on a

24 denaturing polyacrylamide gel system, alongside a synthetic RNA representing the expected

25 processing product. This yielded processing activity, but only when both TOFU-1 and TOFU-2,

26 as well as either SLFL-3 or SLFL-4, were present (**Fig.3b**). Introduction of an E216A mutation

27 into TOFU-2 completely blocked this reaction (**Fig.3b**). Mammalian SLFN nucleases require

28 divalent cations for cleavage activity[34,41]. Likewise, precursor processing was inhibited by

29 EDTA, and was supported by divalent cations like $Mg^{2+}$, $Mn^{2+}$ or $Ca^{2+}$ (at high concentrations),

30 but not by $Zn^{2+}$ (**Suppl. Fig.6a,b**).

31

To exclude the possibility that any BmN4-derived factors were responsible for the cleavage reaction, we also expressed both active and inactive (E216A) minimal versions of the TOFU-1-:TOFU-2:SLFL-3 complex recombinantly in *E. coli* (**Suppl. Fig.5f, g**). This minimal complex was active in precursor cleavage assays, while the E216A mutant was not (**Fig.3c**).

Mature piRNAs carry a monophosphate at their 5' ends, which would be consistent with the cleavage product of a metal-dependent nuclease[34,42]. Successful ligation of the cleavage product to a synthetic RNA oligonucleotide with hydroxyl groups at both 5' and 3' ends confirmed the presence of a 5'-phosphate on the reaction product of the TOFU-1:TOFU-2:SLFL-3 nuclease (**Fig.3d**). Based on these results, we conclude that a complex of TOFU-1, TOFU-2 and either SLFL-3 or SLFL-4 constitutes the enzyme that processes the 5'-end of piRNA precursors in *C. elegans*. We name this complex PUCH for Precursor of 21U RNA 5'-end Cleavage Holoenzyme.

**PUCH is a cap- and sequence-specific ribonuclease**

We probed two key piRNA precursor properties for their relevance to processing. First, piRNA precursors are characterized by a 5'-m7-G Cap[24]. To examine whether the Cap-structure is essential for PUCH activity, we incubated full-length PUCH (isolated by TOFU-2 IP from BmN4 cell extracts) with a precursor having a 5'-phosphate (P) instead of a 5'-m7-G Cap. This experiment revealed that 5'-P precursor RNA was not processed, in contrast to the capped control substrate (**Fig.3e**). A second piRNA-precursor characteristic in *C. elegans* is the presence of a uracil at position three ($U_3$)[24]. This corresponds to the most 5' nucleotide in mature piRNAs, which display an extreme 5'U bias[23]. We tested whether PUCH could process a precursor substrate containing a cytosine at position three (AAC precursor) and found that PUCH did not cleave the AAC precursor at detectable levels (**Fig.3e**). Similar results for Cap- and $U_3$-dependence were obtained with recombinant minimal PUCH complex that only contained the three SLFN domains of TOFU-1, TOFU-2 and SLFL-3 (**Fig.3c**), indicating that these features are recognized directly by the SLFN domains. We conclude that PUCH is a novel type of Cap- and sequence-specific ribonuclease.

**PUCH can cleave PETISCO-bound precursors**

1    *In vivo*, piRNA precursors are bound by PETISCO[4,28], and this enhances piRNA biogenesis. Yet,

2    based on the results described thus far, PUCH does not require PETISCO for activity *in vitro*.

3    PETISCO's main role may therefore be to stabilize precursors *in vivo*, and not to promote

4    PUCH activity. To genetically probe the relationship between PETISCO and PUCH, we asked

5    how the loss of PETISCO function affects precursor accumulation in *tofu-2(e216a)* mutants.

6    To this end, we sequenced small RNAs from a strain carrying the *tofu-2(e216)* allele and

7    lacking the piRNA-specific PETISCO adapter protein PID-1[43]. In *tofu-2(e216a);pid-1(xf35)*

8    double mutants precursor accumulation was reduced (**Fig.4a**), consistent with the idea that

9    PETISCO stabilizes piRNA precursors to allow their processing by PUCH. Mature piRNAs were

10   completely absent, as in *tofu-2(e216a)* single mutants (**Fig.4b**).

11

12   These results also imply that PUCH can process piRNA precursors while they are bound by

13   PETISCO. To test this directly, we first incubated ^{32}P-labelled precursors with purified PETISCO

14   and tested binding in an electromobility-shift-assay (EMSA). We observed that the substrate

15   was indeed bound by PETISCO, resulting in most of the complex not being able to enter the

16   gel, most likely due to the large size of PETISCO (Octameric complex of 240 kDa[28]). The

17   presence of a 5'-m7G-Cap on the precursor enhanced RNA binding by PETISCO (**Suppl. Fig.6c**).

18   Next, we incubated PETISCO-precursor complexes with full-length immunopurified PUCH and

19   analyzed cleavage products in a time-series, which revealed that cleavage is not prevented by

20   the presence of PETISCO (**Fig.4c**). We conclude that PUCH can cleave piRNA precursors, also

21   in presence of PETISCO.

22

23   **PUCH-PETISCO interaction affects precursor processing *in vivo***

24   If PUCH cleaves PETISCO bound precursors, interactions between the two complexes may be

25   expected. However, multiple IP-MS experiments, including coIP of TOFU-2(E216A), did not

26   reveal interactions between PUCH subunits and PETISCO (**Suppl. Fig.1d; Table S1; Table S2**).

27   Reasoning that the presumed interaction may be too transient to be detected in *C. elegans*

28   extracts, we systematically tested interactions between recombinant proteins in pull-down

29   assays. This revealed an interaction between TOFU-1 and the PETISCO complex (**Fig.5a**). Using

30   a combination of pulldown and size exclusion chromatography experiments, we narrowed

31   down the interaction to a short segment of TOFU-1 (residues 82-113, TOFU-1[pep]), just N-

32   terminal to the SLFN domain, and to the extended Tudor (eTudor) domain of the PETISCO

8

1    subunit TOFU-6 (TOFU-6[eTUDOR]) (**Fig.5b**; **Suppl. Fig.7a-e**). Quantitative analysis with the

2    minimal TOFU-1[pep] using isothermal titration calorimetry revealed a $K_d$ of ~20 μM (**Suppl.**

3    **Fig.7f**). We determined the crystal structure of the TOFU-6[eTUDOR]:TOFU-1[pep] complex at 1.7 Å

4    (**Fig.5c; TableS3**). TOFU-1[pep] does not bind TOFU-6[eTUDOR] at the canonical, dimethyl-arginine-

5    binding aromatic cage of the TUDOR domain[44,45], but on the surface of the staphylococcal

6    nuclease-like domain (SN-like domain) of the eTudor domain (**Fig.5c; Suppl. Fig.8a,b**). This

7    region has thus so far not been described to mediate protein-protein interactions. Based on

8    the interaction interface, we designed mutations in both TOFU-1[pep] and TOFU-6[eTUDOR] that

9    should disrupt their interaction and tested these using pull-downs and size exclusion

10    chromatography (**Suppl. Fig.9a-e**). While mutations on only one of the partners (especially

11    TOFU-1[pep]) weakened the interaction, mutation of both partners fully disrupted the

12    interaction. We then tested the same mutations *in vivo*, using Crispr-Cas9 mediated

13    mutagenesis of the endogenous loci, and sequenced piRNAs and their precursors from both

14    single and double mutants. This revealed a reduction of mature piRNAs, as well as an

15    accumulation of precursors, especially in the double mutants (**Fig.5d-f**). We conclude that

16    piRNA accumulation *in vivo* is stimulated by the interaction between PETISCO and PUCH.

17

18    **Discussion**

19    The identification of PUCH completes the piRNA biogenesis toolkit of *C. elegans*. At the

20    sequence level PUCH is unrelated to Zuc, the enzyme that initiates piRNA biogenesis in

21    mammals and flies. Yet, both enzymes perform a similar reaction: they both cleave piRNA

22    precursors at a specified distance from the 5'-end of the precursor. While Zuc depends on

23    Piwi proteins binding precursor 5'-ends[11,13,14], PUCH depends on a 5'-m7G-Cap, which is likely

24    bound by PUCH itself. A second commonality between Zuc and PUCH is the requirement of a

25    uracil downstream of the cleaved phosphodiester bond. While for Zuc this is a rather weak

26    requirement[11], for PUCH this is a prerequisite for cleavage. This imposes a strong selection on

27    potential novel sequences that may evolve towards piRNA precursors. A third similarity

28    between the enzymes is that both contain a transmembrane helix. In case of PUCH, the

29    transmembrane helix is located at the very C-terminus of SLFL-3/4. Even if we did not test the

30    functional relevance of this domain in PUCH yet, Zuc is bound to the mitochondrial outer

31    membrane via its N-terminal transmembrane helix[38,39]. The mere fact that both Zuc and PUCH

32    share this feature suggests convergent evolution of membrane proximity of these enzymes,

9

1   implying that recruitment to a membrane is important for piRNA 5'-end processing *in vivo*.

2   Further experimentation will be required to resolve the role of membrane binding for Zuc and

3   PUCH activity.

4

5   PUCH defines a novel type of ribonuclease, consisting of three subunits, each with one SLFN-

6   like domain. How do our findings relate to SLFN-related proteins in other species? There is a

7   variety of mammalian proteins that contain SLFN-folds. The *Slfn* gene cluster in mice has been

8   described as an immunity locus, displaying high rates of sequence divergence[46]. Interestingly,

9   a parental incompatibility syndrome, Dysdiadochokinesia (DDK) syndrome, has been linked

10  to specific haplotypes of the *Slfn* gene cluster[46]. Given that enzymatic activity of PUCH

11  requires association of three different SLFN-domain containing subunits, one can hypothesize

12  that in mice complexes between distinct paternal and maternal Slfn proteins may form active

13  enzymes, whose activity, or lack thereof, may trigger embryonic lethality. Another study in

14  mice showed that a transposon encoded non-coding RNA inhibits *Slfn* gene expression and

15  thus prevents over-activity of the innate immune system in response to virus infection[47].

16  Moreover, in humans links between immunity and SLFN proteins are known. For instance,

17  SLFN11 restrains translation of viral proteins during HIV infection by cleaving specific tRNAs[48].

18  Interestingly, SLFN11 is a protein with multiple activities. SLFN11 binds single-stranded DNA,

19  and it has been shown to also interfere with replication of certain DNA viruses and to be

20  recruited to stalled replication forks[41]. Furthermore, members of the Orthopoxvirus family,

21  such as the monkeypox virus, contain a virulence factor that carries a single SLFN domain[49,50].

22  Even though the relevance of this specific domain for virulence has not been assessed, a role

23  in host-pathogen interaction control seems likely. Finally, a SLFN-related fold, the Smr

24  domain, has been shown to act as a nuclease in RNA quality control mechanisms, and this

25  function can be traced back to the last universal common ancestor[51].

26

27  Overall, these activities, including the role we identify in piRNA biogenesis, point to a deeply

28  conserved role for Slfn-like domains in immunity- and stress-related mechanisms. Our results

29  show that SLFN domains can form multimeric complexes and that multimerization can unveil

30  highly specific nucleolytic activities. It is conceivable that combinations between proteins with

31  SLFN-related folds may enable uncharacterized activities that help organisms fighting off

32  infectious nucleic acids.

**Acknowledgements**

**Author contributions**

N.P. designed, executed, and analyzed the genetic experiments as well as the RNA binding and cleavage assays.

A.W.B. set up the experiments to produce PUCH complex from BmN4 cells, co-designed the cleavage assays and assisted in data analysis and interpretation.

R.L. Generated expression constructs, purified proteins for biochemical experiments and crystallization trials, performed protein interaction experiments.

S.H. generated *C. elegans* strains through genome editing.

E.N. and F.B. prepared samples for and analyzed them with mass spectrometry and analyzed the results.

T.F. purified proteins, designed and performed protein interaction experiments.

E.K. performed computational analysis of the small RNA data sets and visualized the results.

S.F. performed and interpreted AlphaFold predictions, ITC experiments and all crystallography related work.

R.F.K. assisted in data analysis and interpretation.

The study was conceived and designed by S.F. and R.F.K.

R.F.K., S.F., N.P. and A.W.B. contributed to writing the manuscript and making the figures, with input from all authors.

**Competing interests**

The authors declare no competing interests.

1

2 **Materials and correspondence**

3 Sebastian Falk and René F. Ketting can be approached for materials and correspondence.

4

5 **Methods**

6 **Worm culture**

7 *C. elegans* strains were cultured on OP50 plates according to standard laboratory conditions[52]. For
8 IP/MS experiment worms were grown on high-density egg OP50 plates[53] and transferred to the
9 standard OP50 plates for the last generation. The Bristol N2 strain was used as a reference wild-type
10 strain. Used strains are listed in Table S4.

11

12 **CRISPR/CAS9 mediated genome editing**

13 All protospacers were designed using CRISPOR (http://crispor.tefor.net) and afterwards confirmed
14 with Integrated DNA Technologies "CRISPR-Cas9 guide RNA design checker". Protospacers were
15 cloned to the pRK2412 by SLIM (site directed ligase-independent mutagenesis). The Bristol N2 strain
16 was used for microinjections, unless stated otherwise. ssDNA oligonucleotides (IDT) were utilized as
17 repair template. Each of the repair templates has 35 nucleotides long homology arms. The injection
18 mix contained 50ng/μl guide RNA coding plasmid for the gene of interest; 50ng/μl of plasmid,
19 harboring CAS9 and *dpy-10* (cn64) or *unc-58(e665)* co-conversion guide RNA[54]; 750nM of ssDNA
20 oligonucleotide (repair template for gene of interest) and 750nM of co-conversion ssDNA
21 oligonucleotide. Used protospacers and repair templates are listed in the Table S4.

22

23 **Crosses with piRNA sensor**

24 RFK1059 (*tofu-2*[E216A]) and *slfl-3(xf248)* mutant hermaphrodite worms were crossed with males of
25 the RFK1246 strain, which carries a *mut-7* deletion as well as the piRNA sensor[22]. Worms, carrying
26 piRNA sensor and *tofu-2[E216]* or *slfl-3(xf248)* mutation, and wild type for *mut-7* were selected by
27 genotyping. Genotyping primers can be found in Table S4.

28

29 **Microscopy**

30 Images of piRNA sensor carrying strains were obtained using a Leica DM6000B. Young adults and adult
31 worms were washed in a drop of M9 (22mM $KH_2PO_4$, 42mM $Na_2HPO_4$, 85mM NaCl, 1mM $MgSO_4$) and
32 immobilized with 30mM sodium azide in M9 buffer. Imaging of Bm4 cells were done using Leica TCS
33 SP5. Images were processed using ImageJ and Adobe Illustrator.

34

35 **Mass spectrometry**

36 *Worm pellet preparation*

37 All IP/MS experiments were performed in quadruplicates. Worms, grown on the OP50 plates were
38 bleached (2% NaClO, 666mM NaOH) into high-density egg plates, grown until gravid adult stage and
39 bleached again. The embryos were left to hatch in M9 buffer (22mM $KH_2PO_4$, 42mM $Na_2HPO_4$, 85mM
40 NaCl, 1mM $MgSO_4$), L1 stage worms were seeded on standard OP50 plates and harvested at young
41 adult stage. Worms were washed three times with M9 buffer and one time with cold sterile water.
42 200μl worm aliquots were pelleted and frozen in liquid nitrogen and stored at −80°C.

43 *Lysis preparation*

1. 200 µl of synchronized young adult worms were thawed on ice and resuspended in 250 µl of 2x Lysis
2. Buffer (50mM Tris HCl pH7.5, 300 mM NaCl, 3mM $MgCl_2$, 2mM DTT, 2mM Triton X100, 2x cOmplete
3. Mini, EDTA-free, Roche, 11836170001) and 50µl of sterile water. The Bioruptor Plus (Diagenode)
4. sonicator was used to lyse worms (10 cycles 30/30 seconds, high energy, 4°C). After pelleting, the
5. supernatant was accurately removed without the lipid phase. Finally, the protein concentration of the
6. lysate was determined using Pierce BCA Protein Assay Kit (ThermoFisher Scientific, 23225).
7. *Immunuoprecipitation*
8. For anti-HA IPs, 550µL of worm lysate containing 0,75mg protein was resuspended in a final volume
9. of 550µL of 1x Lysis Buffer. Anti-HA IPs were performed with 2µg of in-house made anti-HA antibodies
10. (mouse, clone 12CA5). The lysate was incubated with the antibodies for two hours at 4°C. For each
11. sample, 30µl of protein G magnetic beads (Dynabeads, Invitrogen) were washed three times in
12. washing buffer (25mM Tris HCl pH7.5, 150mM NaCl, 1.5mM $MgCl_2$, 1mM DTT, 1mM Triton X100,
13. cOmplete Mini, EDTA-free, Roche, 11836170001). Subsequently, equilibrated beads were added to
14. the lysis and incubated for an additional hour at 4°C by end-over-end rotation. Finally, beads were
15. washed 6 times with Wash Buffer, resuspended in 2xNuPAGE LDS Sample Buffer (containing 200mM
16. DTT) and boiled for 15min at 95°C.
17. To identify of TOFU-2::HA and TOFU-2::HA(E216A), samples were separated on a 4%–12% NOVEX
18. NuPAGE gradient SDS gel (Thermo) for 10 min at 180 V in 1× MES buffer (Thermo). Proteins were
19. fixated and stained with Coomassie G250 Brilliant Blue (Carl Roth). The gel lanes were cut, minced into
20. pieces, and transferred to an Eppendorf tube. Gel pieces were destained with a 50% ethanol/ 50mM
21. ammonium bicarbonate (ABC) solution. Proteins were reduced in 10mM DTT (Sigma-Aldrich) for 1h at
22. 56°C and then alkylated with 5mM iodoacetamide (Sigma-Aldrich) for 45 min at room temperature.
23. Proteins were digested with trypsin (Sigma) overnight at 37°C. Peptides were extracted from the gel
24. by two incubations with 30% ABC/acetonitrile and three subsequent incubations with pure
25. acetonitrile. The acetonitrile was subsequently evaporated in a concentrator (Eppendorf) and loaded
26. on StageTips[55] for desalting and storage.
27. For mass spectrometric analysis, peptides were separated on a 20-cm self-packed column with 75µm
28. inner diameter filled with ReproSil-Pur 120 C18-AQ (Dr.Maisch GmbH) mounted to an EASY HPLC 1000
29. (Thermo Fisher) and sprayed online into an Q Exactive Plus mass spectrometer (Thermo Fisher). We
30. used a 94-min gradient from 2 to 40% acetonitrile in 0.1% formic acid at a flow of 225nl/min. The mass
31. spectrometer was operated with a top 10 MS/MS data-dependent acquisition scheme per MS full
32. scan. Mass spectrometry raw data were searched using the Andromeda search engine[56] integrated
33. into MaxQuant suite 1.6.5.0[57] using the UniProt *C. elegans* database (August 2014; 27,814 entries). In
34. both analyses, carbamidomethylation at cysteine was set as fixed modification, while methionine
35. oxidation and protein N-acetylation were considered as variable modifications. Match-between-run
36. option was activated. Prior to bioinformatic analysis, reverse hits, proteins only identified by site,
37. protein groups based on one unique peptide, and known contaminants were removed.
38. For the further bioinformatic analysis, the LFQ values were log2-transformed and the median across
39. the replicates was calculated. This enrichment was plotted against the – log 10- transformed P value
40. (Welch's t-test) using the ggplot2 package in the R environment.
41.
42. **Western blot from the worm lysis**
43. Worms were grown and lysed as described for the Mass spectrometry section. Lysis of both RFK1269
44. and RFK1280 worms, containing 15µg of protein, were mixed with 2x gel loading buffer (2x Novex
45. NuPage LDS sample buffer (Invitrogen), supplemented with 200mM DTT) and were heated at 95°C for

1   10min prior to resolving on a 4-12% Bis-Tris NuPage NOVEX gradient gel (Invitrogen) in 1x Novex
2   NuPAGE MOPS SDS Running Buffer (Invitrogen) at 150 V. Separated proteins were transferred to
3   nitrocellulose membrane (Amersham) 1h at 120V using 1x NuPAGE Transfer Buffer (Invitrogen)
4   supplemented with 10% methanol. The membrane was incubated for 30min in 1x PBS-Tween (0.05%)
5   supplemented with 5% skim milk, cleaved and incubated overnight with primary antibodies diluted in
6   PBS-Tween (1:1,000 monoclonal anti-HA (12CA5, in-house); 1:1,000 anti-h3 (H0164, Sigma) rabbit
7   polyclonal antibodies. Subsequently, the membrane was washed 5 times for 5min in PBS-Tween, prior
8   to incubation with the secondary antibody, using 1:10,000 horse anti-mouse HRP-linked antibody
9   (#7076, Cell Signaling) and goat anti-rabbit HRP-linked antibodies (#7074, Cell Signaling) and imaged
10  using SuperSignal™ West Pico Plus (TermoFischer) kit.
11
12  **RNA isolation and RNA sequencing**
13  Worms were grown at 20°C, synchronized by bleaching (2% NaClO, 666mM NaOH) and were left to
14  hatch overnight in M9 buffer. Next, L1-stage worms were seeded onto OP50 plates and harvested as
15  young adults. For RNA extraction 500 µL of TRISOL LS (ThermoFisher Scientific, 10296-028) was added
16  to the 50µL worm aliquot, and five cycles of freezing in liquid nitrogen/thawing in the 37°C water bath
17  were performed. Samples were centrifuged for 5min at 21x$g$ at RT, and supernatant was collected. 1
18  volume of 100% EtOH was added to the supernatant, before proceeding with the RNA extraction using
19  the Direct-zol™ RNA MicroPrep (Zymo) kit. RNA was eluted into 13µl of Nuclease Free water (Ambion®
20  Invitrogen™) and each sample was divided into two aliquots for piRNA-precursor and mature piRNA
21  library preparation.
22  *CIP/RppH treatment and library preparation (for precursors).*
23  CIP treatment on 1,5µg of isolated RNA was performed in rCutSmart™ Buffer (B6004S) using 3µL of
24  Quick CIP (M0525L) in a 40µL reaction. The reaction was incubated at 37°C for 20min, followed by
25  heat inactivation for 2min at 80°C. The CIP-treated RNA was subjected to another round of purification
26  using the Direct-zol™ RNA MicroPrep (Zymo) kit. RppH (NEB) treatment was performed with a starting
27  amount of 500ng.
28  *Library preparation, sequencing and analysis.*
29  NGS library prep was performed with NEXTflex Small RNA-Seq Kit V3 following Step A to Step G of Bioo
30  Scientific`s standard protocol. Amplified libraries were purified by running an 8% TBE gel and size-
31  selected for 15-40 nt. Libraries were profiled in a High Sensitivity DNA Chip on a 2100 Bioanalyzer
32  (Agilent technologies), quantified using the Qubit dsDNA HS Assay Kit, in a Qubit 2.0 Fluorometer (Life
33  technologies) and sequenced on Illumina NextSeq 500/550.
34  The raw sequence reads in FastQ format were cleaned from adapter sequences and size-selected for
35  18-35 nt inserts (plus 8 random adapter bases) using cutadapt v.4.0 (http://cutadapt.readthedocs.org)
36  with parameters "-a TGGAATTCTCGGGTGCCAAGG -m 26 -M 43". Data quality was assessed with
37  FastQC v.0.11.9 (https://github.com/s-andrews/FastQC) and MultiQC v.1.9 (https://multiqc.info/).
38  Read alignment to the *C. elegans* genome (Ensembl WBcel235/ce11 assembly) with concomitant
39  trimming of the 8 random bases was performed using Bowtie v.1.3.1 (http://bowtie-
40  bio.sourceforge.net) with parameters "-v 1 -M 1 -y --best --strata --trim5 4 --trim3 4 -S" and the SAM
41  alignment files were converted into sorted BAM files using Samtools v.1.10 (http://www.htslib.org).
42  *C. elegans* WBcel235/ce11 gene annotation in GTF format was downloaded from Ensembl release 96
43  (ftp://ftp.ensembl.org/pub/). Aligned reads were assigned to small RNA loci and classes using
44  Samtools, GNU Awk and Subread featureCounts v.1.6.2 (http://bioinf.wehi.edu.au/featureCounts/).
45  Structural reads aligned in sense orientation to rRNA, tRNA, snRNA and snoRNA loci were excluded

1    from further analysis. Mature piRNAs were stringently defined as reads of length 21nt starting with T
2    and fully overlapping with annotated piRNA (21ur) genes in sense orientation. Because 21ur gene
3    annotation corresponds to mature piRNA sequences, piRNA precursors were stringently defined as
4    reads of length 23-35 nt starting 2 bp upstream of the annotated 5'-end of (mature) piRNAs in sense
5    orientation. The relative abundance of mature and precursor piRNAs was normalized to the number
6    of non-structural 18-35 nt reads in each sample. Coverage tracks of aligned reads overlapping in sense
7    with piRNA genes were produced using Bedtools v.2.27.1 (http://bedtools.readthedocs.io) and
8    kentUtils v.385 (https://github.com/ucscGenomeBrowser/kent). The tracks were normalized based
9    on all non-structural reads in each sample and visualized on the IGV genome browser v.2.15.4
10    (https://igv.org/).
11

12 **3' RNA radioactive labeling**
13    3'-end labeling of substrate RNA (see Table S4 for sequence) was performed in a 25µL reaction
14    containing 2.5µL f DMSO, 2.5µL of T4 ligase buffer (NEB), 1µL of T4 ligase (NEB), 2.5µL 10mM ATP
15    (NEB), 1µL of synthetic RNA precursor (5pmol/µL). The reaction was mixed and and 2.5µL of [5'-
16    $^{32}$P]pCp (SCP-111, Hartmann analytic) was added before overnight incubation at 16°C. Finally, the
17    labeled RNA was purified using G25 columns (Cytiva) according to the manufacturer's protocol. The
18    3'-end labeled synthetic RNA precursor was used for *in vitro* cleavage assays and in EMSAs.
19

20 **5' RNA radioactive labeling**
21    5pmol synthetic RNA oligonucleotide was labeled with ATP, [γ-$^{32}$P] (PerkinElmer) using T4 PNK(NEB),
22    according to the manufacturer's protocol. The sequences of the RNA substrates can be found in Table
23    S4.
24

25 **Plasmids**
26    Full-length CeTOFU-2 was amplified from N2 cDNA and was inserted by restriction-based cloning into
27    the pBEMBL vector (kind gift of R.Pillai) in which expression of a N-terminal eGFP tag is driven by the
28    OpIE2 promoter. Likewise, CeTOFU-1 was inserted into a vector harboring a C-terminal 3xFLAG-
29    mCherry cassette. CeSLFL3 and CeSLFL4 were inserted into a vector backbone containing an N-
30    terminal HA tag. All primers, vector backbones and detailed cloning strategies can be found in
31    Supplemental Materials.
32

33 **BmN4 cell culture and transfection**
34    BmN4 cells were cultured at 27°C in IPL-41 insect medium (Gibco) supplemented with 10% FBS and
35    0.5% Pen-Strep (Gibco). 24 hours prior to transfection, ~4x 10ˆ6 cells were seeded in a 10-cm dish
36    (using one 10-cm dish for each condition in the cleavage reaction). Cells were transfected with 10 µg
37    of each plasmid DNA using XtremeGene HP (Roche) transfection reagent, according to the
38    manufacturer's instructions. 72h post transfection cells were harvested, washed twice in ice-cold PBS
39    and pelleted by centrifugation at 500xg for 5min at 4°C.
40

41 **GFP-IP from BmN4 cells**
42    Roughly 4 x 10ˆ6 BmN4 cells were harvested from each 10-cm dish (see above), washed once in 5mL
43    ice-cold PBS and once more in 1 mL ice-cold PBS. Subsequently, cells were pelleted by centrifugation
44    for 5min at 500xg at 4°C and frozen at -80°C. Directly before use, BmN4 cell pellets were thawn on ice
45    and lysed in 1 mL IP-150 Lysis Buffer (30mM Hepes [pH7.4], 150mM KOAc, 2mM Mg(OAc)$_2$ and 0.1%

1     Igepal freshly supplemented with EDTA-free protease inhibitor cocktail and 5mM DTT) for 1 hour by
2     end-over-end rotation at 4°C. Cells were further lysed by passing the lysate ten times through a 20-
3     gauge syringe needle followed by five passes through a 30-gauge needle. Cell debris was pelleted by
4     centrifugation at 17,000xg for 20min at 4°C. Supernatant fractions were collected and subjected to
5     GFP-IP using GFP-Trap beads (Chromotek). The GFP-Trap beads (15µL beads suspension per reaction)
6     were washed 3 times in 1mL of IP-150 Lysis Buffer. Equilibrated beads were subsequently incubated
7     with the BmN4 cell lysate and incubated overnight by end-over-end rotation at 4°C. The next day,
8     immunoprecipitated complexes were washed five times using 1mL of IP-150 Lysis Buffer and were
9     subsequently used for *in vitro* cleavage assays or for immunodetection using Western Blot analysis.
10
11    **Western Blot**
12    Samples were prepared in 1x Novex NuPage LDS sample buffer (Invitrogen) supplemented with
13    100mM DTT and were heated at 95°C for 10min prior to resolving on a 4-12% Bis-Tris NuPage NOVEX
14    gradient gel (Invitrogen) in 1x Novex NuPAGE MOPS SDS Running Buffer (Invitrogen) at 140V.
15    Separated proteins were transferred to nitrocellulose membrane (Amersham) overnight at 20V using
16    1x NuPAGE Transfer Buffer (Invitrogen) supplemented with 10% methanol. The next day, the
17    membrane was incubated for 1h in 1x PBS-Tween (0.05%) supplemented with 5% skim milk and
18    incubated for 1 hour with primary antibodies diluted in PBS-Tween (1:1,000 monoclonal anti-Flag M2,
19    F3165, Sigma-Aldrich; 1:1,000 monoclonal anti-GFP antibodies (B-2), Santa Cruz, sc-9996, K1115;
20    1:1,000 monoclonal anti-HA (12CA5, in-house); 1:1,000 anti-actin (A5060) rabbit monoclonal
21    antibodies, Sigma. Subsequently, the membrane was washed 3 times for 5min in PBS-Tween, prior to
22    incubation with the secondary antibody, using 1:10,000 IRDye 800CW Goat anti-mouse and IRDye
23    680LT Donkey anti-rabbit IgG (LI-COR) and imaged on an Odyssey CLx imaging system (LI-COR).
24
25    ***In vitro* cleavage assay.**
26    The PUCH complex used for *in vitro* cleavage assays was obtained in two different ways. The full-length
27    PUCH complex was obtained from GFP-IPs using BmN4 cell lysates (see above), whereas the minimal
28    catalytic complex (mini-PUCH) was purified from *E.coli.*
29    For the *in vitro* cleavage assays performed with IP material from BmN4 cells, beads were washed in
30    the cleavage buffer (CB) containing 40mM Tris-HCl, pH 8.0, 20mM KCl, 11mM $MgCl_2$ and 2mM DTT.
31    Beads were subsequently resuspended in 10µL of CB and incubated with 0.2pmol of the labeled RNA
32    substrate for 1h at room temperature.
33    For cleavage assays with mini-PUCH purified from *E.coli* 0.2pmol of labeled RNA substrate was
34    incubated in 10µL CB buffer with 27nM mini-PUCH protein complex (final concentration) at 20°C for
35    30min.
36    The cleavage reaction was terminated by adding 1µL of 20mg/ml proteinase K. 1 volume of the 2xRNA
37    Gel Loading Dye (Thermo Scientific™, R0641) was added and the RNA was resolved on a 15% TBE-
38    UREA gel (Novex™) for 90min at 180V with 1xTBE as the running buffer.
39    *Substrate specificity test of PUCH complex*
40    Capped RNA oligonucleotides were labeled at the 3'end, 0.2pmol (1µL) of RNA per sample were used
41    in the cleavage reaction. For reaction with IP material, to obtain 5'P-containing piRNA precursor
42    oligonucleotide, 5'OH-piRNA precursor had been labeled on the 3'end as described above. After
43    labeling, 5'P was created by T4 PNK treatment (NEB, M0201S), done according to the NEB T4 PNK
44    protocol. For the reaction with mini-PUCH 5'OH-piRNA precursor oligonucleotide had been labeled on
45    the 5'end as described above.

1  *Analysis of divalent cations as cofactor of PUCH complex*

2  For the metal assay, beads were washed with CB, but 100mM $MgCl_2$ was replaced by $ZnCl_2$, $MnCl_2$ or

3  $CaCl_2$. Cleavage reaction was done with full-length PUCH obtained from GFP-IP material from BmN4

4  cell lysates.

5  *Ligation of small RNA oligo to the cleavage product in order to prove formation of 5'P on the cleaved*

6  *RNA precursor*

7  2pmol of labeled RNA was incubated in 35µL of CB containing mini-PUCH (or mutated mini-PUCH) at

8  a final concentration of 40nM and was incubated at 20°C for 1h. Afterwards 3 volumes of Trisol LS

9  reagent (ThermoFisher Scientific, 10296-028) was added, and RNA was purified using Direct-zol™ RNA

10  MicroPrep (Zymo) according to the manufacturer's protocol. Next, the RNA was ligated to 10pmol of

11  5'OH-rGrUrCrUrGrUrUrUrArA-OH3' oligonucleotide using T4 RNA ligase according to the

12  manufacturer's protocol. After 16h of incubation at 16°C, the reaction terminated by proteinase K and

13  RNA was resolved on a 15% TBE-UREA gel (Novex™) for 90min at 180V with 1xTBE as the running

14  buffer.

15  *PUCH complex cleavage activity in presence of PETISCO*

16  The assay has been done with PUCH complex, obtained from Bm4 cells. Per sample: 1µL of 3'end

17  labeled piRNA precursor (0.2pmol) was incubated with five times access of PETISCO protein complex

18  on ice for 1h in 10µL of CB buffer. PUCH-IP containing beads were resuspended in 10µL of RNA-

19  PETISCO mix and incubated at 20°C.

20

21  **EMSA**

22  0.2pmol of capped piRNA precursor, 5'P piRNA precursor and 5'OH-piRNA precursor were incubated

23  with recombinant proteins of PETISCO complex, containing IFE-3, TOFU-6, ERH-2 and PID-3[28] in a

24  concentration range from 75pM to 1.44µM, in 10µL of binding buffer (20mM HEPES pH7.5, 150mM

25  NaCl) for 1h at the room temperature. After the incubation, each sample was mixed with 15% Ficoll

26  with bromophenol blue. Native 6% TBE gel was pre-run for 30min at 180V at room temperature in

27  1xTBE, and samples were resolved for 2h.

28

29  **Recombinant protein production in *E. coli***

30  PETISCO and its subunits (IFE-3, TOFU-6, PID-3, ERH-2) were purified and reconstituted as described

31  in[28]. Using ligation-independent cloning, genes encoding TOFU-1, TOFU-2, and SLFL-3 were cloned into

32  modified pET vectors. All proteins were produced as an N-terminal His-Tagged fusion protein with

33  varying fusion tags that can be removed by the addition of 3C protease. Proteins or protein complexes

34  were produced in the *E. coli* BL21(DE3) derivate strains in terrific broth medium. Briefly, cells were

35  grown at 37°C, and when the culture reached an optical density (OD) at 600 nm of 2-3, the

36  temperature was reduced to 18°C. After 2h at 18°C, 0.2mM IPTG was added to induce protein

37  production for 12-16 h overnight.

38

39  **Co-expression pull-down assays**

40  For interaction studies by the co-expression co-purification strategy, two plasmids containing the gene

41  of interest and different antibiotic resistance markers were co-transformed into BL21(DE3) derivative

42  strains to allow co-expression. 50 mL of cells were grown in TB medium shaking at 37°C, and when the

43  culture reached an OD at 600 nm of 2-3, the temperature was reduced to 18°C. Protein production

44  was induced after 2 h at 18°C, through the addition of 0.2 mM IPTG for 12-16 h overnight. Cells were

45  harvested by centrifugation and the cell pellets were resuspended in 2 mL of lysis buffer (50 mM

1  Sodium phosphate, 20 mM Tris/HCl, 250 mM NaCl, 10 mM Imidazole, 10% (v/v) glycerol, 0.05% (v/v)
2  NP-40, 5 mM 2-mercaptoethanol pH 8.0) per gram of wet cell mass. Cells were lysed by ultrasonic
3  disintegration, and insoluble material was removed by centrifugation at 21,000xg for 10 min at 4°C.
4  For Streptactin pull-downs, 500 µL of supernatant was applied to 20 Strep-Tactin®XT resin (IBA
5  Lifesciences); for MBP pull-downs, 500 µL supernatant was applied to 20 µL amylose resin (New
6  England Biolabs) and incubated for two hours at 4°C. Subsequently, the resin was washed three times
7  with 500 µL of lysis buffer. The proteins were eluted in 50 µL of lysis buffer supplemented with 10 mM
8  maltose or 50 mM biotin in the case of amylose beads or Strep-Tactin®XT beads, respectively. Input
9  material and eluates were analyzed by SDS–PAGE and Coomassie brilliant blue staining.
10

11 **Pull-down assays with purified proteins**
12 To analyze protein interaction with purified proteins, appropriate protein mixtures (bait 10-20 µM,
13 prey in 1.2-fold molar excess) were incubated in binding buffer containing 20 mM Tris/HCl (pH 7.5),
14 150 mM NaCl, 10% (v/v) glycerol, 0.05% (v/v) NP40, 1 mM DTT for 30min at 4°C. Subsequently, the
15 indicated beads were added to the protein mixtures were then incubated with the indicated beads for
16 2 h on ice: Glutathione sepharose beads (Cube Biotech), Amylose sepharose beads (New England
17 Biolabs)), and Strep-Tactin XT beads (IBA). Subsequently, the beads were washed three times with 200
18 µL mL binding buffer, and the retained material was eluted with 0.05 mL incubation buffer
19 supplemented with 20 mM of reduced glutathione, 10 mM maltose, or 50 mM biotin. Input material
20 and eluates were analyzed by SDS–PAGE and Coomassie brilliant blue staining.
21

22 **Purification of the trimeric mini PUCH**
23 To reconstitute minimal PUCH, TOFU-1 (residues 160 to 373), TOFU-2 (residues 200-433) and SLFL-3
24 (residues 1-345) were co-expressed in BL21 (DE3). In case of inactive minimal PUCH, an inactive TOFU-
25 2 mutant (residues 200-433, E216A) was used. TOFU-1 carried an N-terminal His10-MBP tag, TOFU-2
26 an N-terminal His10-MBP and a C-terminal StrepII tag, and SLFL-3 an N-terminal His6-GST tag. Cells
27 were grown at 37°C, and when the culture reached an optical density (OD) at 600 nm of 2-3, the
28 temperature was reduced to 18°C. After 2 h at 18°C, 0.2 mM IPTG was added to induce protein
29 production for 12-16 h overnight. All purification steps were performed on ice or at 4°C. Cells were
30 lysed by sonication in lysis buffer (50 mM Sodiumphosphate, 20 mM Tris/HCl, 500 mM NaCl, 20 mM
31 imidazole, 10% (v/v) glycerol, and 5 mM 2-mercaptoethanol at pH 8.0). PUCH was purified by
32 immobilized metal affinity chromatography (IMAC) using a 5 mL Ni2+-chelating HisTrap FF column
33 (Cytiva). Proteins were eluted with lysis buffer supplemented with 500 mM imidazole and dialyzed
34 overnight against 20 mM Tris/HCl, 150 mM NaCl, 10% (v/v) glycerol, and 5 mM 2-mercaptoethanol at
35 pH 7.5. After dialysis, PUCH was subjected to heparin affinity chromatography on a 5 mL HiTrap
36 Heparin HP (Cytiva) followed by size exclusion chromatography on a HiLoad Superdex 200 16/600
37 (Cytiva) in 20 mM Tris/HCl pH 7.5, 150 mM NaCl, 10% (v/v) glycerol, 2 mM DTT.
38

39 **Analytical size exclusion chromatography**
40 Purified proteins were incubated alone or in different mixtures in concentrations between 20-40 µM
41 (total volume of 50 µl) in size exclusion buffer (20 mM Tris/HCl pH 7.5, 150 mM NaCl, 2 mM DTT) as
42 indicated in the figure legends. Samples were incubated for 1 h on ice to allow complex formation.
43 Complex formation was assayed by comparing the elution volumes in SEC on a Superdex 200 Increase
44 3.2/300 (Cytiva). The SEC peak fractions were analyzed by SDS–PAGE and visualized by Coomassie
45 brilliant blue staining.

**Isothermal titration calorimetry**

ITC experiments to quantitatively analyze the interaction between TOFU-1 peptide (residues 82-113) and the TOFU-6 eTUDOR domain (residues 119-314) interaction were carried out using the PEAQ-ITC Isothermal titration calorimeter (Malvern). The TOFU-1 82-113 peptide does not contain Tyrosine or Tryptophane residues. To be able to determine the concentration precisely, we engineered a TOFU-1 peptide (TOFU-1[W-82-113]) that contains a Tryptophan residue at the N-terminus. Data processing and analysis was performed using the PEAQ-ITC software (Malvern). Before the measurements, the samples were dialyzed overnight simultaneously against 1 L of ITC buffer (20 mM Tris, 250 mM NaCl, 0.5 mM TCEP, pH 7.50). TOFU-1[W-82-113] (the reactant) samples were concentrated to 45-48 µM and TOFU-6[eTUDOR] (the injectant) to 400-450 µM. Titrations were carried out at 25°C with 2 µL of the injectant per injection added to 200 µL of reactant cell solution. The reported Kd and stoichiometry are the average of three experiments, and the reported experimental error is the standard deviation.

**TOFU-6[eTUDOR] TOFU-1[pep] crystallization**

Purified TOFU-6[eTUDOR] and TOFU-1[W-82-113] were mixed with TOFU-1[W-82-113] being in 1.5-fold molar excess and subjected to size exclusion chromatography on a HiLoad Supdersex S75 16/600 (Cytiva) equilibrated in 20 mM Tris/HCl, 150 mM NaCl, 2 mM DTT pH7.5. The complex containing fractions were concentrated to 10 mg/ml by ultrafiltration. Crystallizsation trials were performed at 4°C and 22°C at 8-10 mg/ml using a vapor diffusion set-up. Drops were setup using a mosquito® Crystallization Robot (SPT Labtech) on 96-Well 2-Drop MRC Crystallization Plates (Swissci) by mixing the protein complex and crystallization solution in a 200:200 nl and 400 :200 nl ratio.

Small crystals grew at 4°C in various conditions of the Morpheus Screen[58]. Several rounds of microseed matrix screening yielded larger crystals. The best crystals grew in 0.2 M Na bromide, 0.1 M Bis Tris propane pH 7.5, 20% (w/v) PEG 3350 at 22°C in the PACT screen[59]. Crystals were soaked with a mother liquor supplemented with 20% (v/v) glycerol for cryoprotection and then frozen in liquid nitrogen.

**Data collection, structure determination and refinement**

Data were collected at the ESRF (Grenoble, France) beamline ID30A-3 on September 26th 2021; https://doi.esrf.fr/10.15151/ESRF-DC-1033968485.

Data were processed with autoPROC[60] using XDS[61] and AIMLESS[62]. Phases were determined by molecular replacement using the AlphaFold model of the *C. elegans* TOFU-6 eTUDOR domain (residues 120-314) (https://alphafold.ebi.ac.uk/entry/Q09293). Molecular replacement was performed with Phaser[63] within Phenix[64]. The model was processed with Phenix (process predicted model) to translate the pLDDT values to B factors and to remove flexible regions. Following molecular replacement, the model was automatically built with Buccaneer[65], manually completed with COOT[66] and refined using phenix.refine[67]. Model quality was assessed using molprobity[68] and PDB-REDO[69]. The refined model has a clashscore of 5.06 and 98.54% of the residues fall into Ramachandran favored and 1.46% into Ramachandran allowed regions. Data collection and refinement statistics are listed in Supplemental Table S3. Molecular graphics of the structures were prepared using UCSF ChimeraX[70]. Coordinates and structure factors have been deposited in the Protein Data Bank with accession codes PDB ID 8BY5.

**Protein complex structure prediction with AlphaFold2 multimer**

The prediction of protein complex structures was performed using AlphaFold v2.1.0 on the Colab notebook (ColabFold)[71]:

1    https://colab.research.google.com/github/sokrypton/ColabFold/blob/main/AlphaFold2.ipynb

2    The following settings were used: template_mode (none), msa_mode (MMSeq2

3    (UniRef+Environmental), pair_mode (unpaired + paired), model_type (AlphaFold2-multimer-v2). In

4    case of the tetrameric PUCH 3 recycles were used, for the trimeric PUCH, 48 recycles were used.

5    Protein sequences were obtained from Uniprot and for initial complex predictions, full-length

6    sequences from all four proteins (TOFU-1, TOFU-2, SLFL-3, and SLFL-4) were used. The predicted

7    models and the predicted alignment error (PAE) score were visualized and analyzed using ChimeraX[70].

8    Predicted complexes either contained SLFL-3 or SLFL-4. As SLFL-3 and SLFL-4 are paralogs that are 90%

9    identical and 93% similar on the protein sequence level, we focused on predictions of the trimeric

10    PUCH containing TOFU-1, TOFU-2 and SLFL-3. For the prediction of the core PUCH the following

11    residue boundaries were used. TOFU-1 residues 156-373, encompassing the SLFN domain with an N-

12    terminal extension. TOFU-2 residues 200-433, encompassing the SLFN domain and two C-terminal

13    alpha helices. SLFL-3 residues 103-300, encompassing the SLFN domain.

14

15    **Data availability**

16    Sequencing data is available at NCBI's Sequence Read Archive under accession number PRJNA925182

17    (https://dataview.ncbi.nlm.nih.gov/object/PRJNA925182?reviewer=951lavsn8a0umpj5j17m8bk738).

18    The mass spectrometry proteomics data have been deposited to the ProteomeXchange Consortium

19    via the PRIDE[72] partner repository with the dataset identifier PXD039502.

20    Username: reviewer_pxd039502@ebi.ac.uk

21    Password: T2C6anBX

22    Coordinates and structure factors of the TOFU-6$^{eTUDOR}$ TOFU-1$^{pep}$ complex structure have been

23    deposited in the Protein Data Bank with accession codes PDB ID 8BY5.

24

25    **Code availability**

26    Codes can be obtained upon reasonable request from the corresponding authors.

27

28    **References**

29    1.    Wells, J. N. & Feschotte, C. A Field Guide to Eukaryotic Transposable Elements. *Annu*

30          *Rev Genet* **54**, 539–561 (2020).

31    2.    Ozata, D. M., Gainetdinov, I., Zoch, A., O'Carroll, D. & Zamore, P. D. PIWI-interacting

32          RNAs: small RNAs with big functions. *Nat Rev Genet* **20**, 89–108 (2019).

33    3.    Czech, B. *et al.* piRNA-Guided Genome Defense: From Biogenesis to Silencing. *Annu*

34          *Rev Genet* **52**, 131–157 (2018).

35    4.    Cordeiro Rodrigues, R. J. *et al.* PETISCO is a novel protein complex required for 21U

36          RNA biogenesis and embryonic viability. *Genes Dev* **33**, (2019).

37    5.    Jo, U. & Pommier, Y. Structural, molecular, and functional insights into Schlafen

38          proteins. *Exp Mol Med* **54**, 730–738 (2022).

39    6.    Cosby, R. L., Chang, N.-C. & Feschotte, C. Host-transposon interactions: conflict,

40          cooperation, and cooption. *Genes Dev* **33**, 1098–1116 (2019).

41    7.    Wu, P.-H. & Zamore, P. D. Defining the functions of PIWI-interacting RNAs. *Nat Rev*

42          *Mol Cell Biol* **22**, 239–240 (2021).

43    8.    Luteijn, M. J. & Ketting, R. F. PIWI-interacting RNAs: From generation to

44          transgenerational epigenetics. *Nat Rev Genet* **14**, (2013).

9.  Voigt, F. *et al.* Crystal structure of the primary piRNA biogenesis factor Zucchini reveals similarity to the bacterial PLD endonuclease Nuc. *RNA* **18**, 2128–34 (2012).

10. Ipsaro, J. J., Haase, A. D., Knott, S. R., Joshua-Tor, L. & Hannon, G. J. The structural biochemistry of Zucchini implicates it as a nuclease in piRNA biogenesis. *Nature* **491**, 279–83 (2012).

11. Izumi, N., Shoji, K., Suzuki, Y., Katsuma, S. & Tomari, Y. Zucchini consensus motifs determine the mechanism of pre-piRNA production. *Nature* **578**, 311–316 (2020).

12. Nishimasu, H. *et al.* Structure and function of Zucchini endoribonuclease in piRNA biogenesis. *Nature* **491**, 284–7 (2012).

13. Mohn, F., Handler, D. & Brennecke, J. Noncoding RNA. piRNA-guided slicing specifies transcripts for Zucchini-dependent, phased piRNA biogenesis. *Science* **348**, 812–817 (2015).

14. Han, B. W., Wang, W., Li, C., Weng, Z. & Zamore, P. D. Noncoding RNA. piRNA-guided transposon cleavage initiates Zucchini-dependent, phased piRNA production. *Science* **348**, 817–21 (2015).

15. Tang, W., Tu, S., Lee, H.-C., Weng, Z. & Mello, C. C. The RNase PARN-1 Trims piRNA 3' Ends to Promote Transcriptome Surveillance in C. elegans. *Cell* **164**, 974–84 (2016).

16. Montgomery, T. A. *et al.* PIWI associated siRNAs and piRNAs specifically require the Caenorhabditis elegans HEN1 ortholog henn-1. *PLoS Genet* **8**, (2012).

17. Billi, A. C. *et al.* The caenorhabditis elegans HEN1 Ortholog, HENN-1, methylates and stabilizes select subclasses of germline small RNAs. *PLoS Genet* **8**, (2012).

18. Kamminga, L. M. *et al.* Differential impact of the HEN1 homolog HENN-1 on 21U and 26G RNAs in the germline of Caenorhabditis elegans. *PLoS Genet* **8**, (2012).

19. Wang, G. & Reinke, V. A C. elegans Piwi, PRG-1, regulates 21U-RNAs during spermatogenesis. *Curr Biol* **18**, 861–7 (2008).

20. Batista, P. J. *et al.* PRG-1 and 21U-RNAs interact to form the piRNA complex required for fertility in C. elegans. *Mol Cell* **31**, 67–78 (2008).

21. Das, P. P. *et al.* Piwi and piRNAs Act Upstream of an Endogenous siRNA Pathway to Suppress Tc3 Transposon Mobility in the Caenorhabditis elegans Germline. *Mol Cell* **31**, (2008).

22. Bagijn, M. P. *et al.* Function, targets, and evolution of Caenorhabditis elegans piRNAs. *Science* **337**, 574–578 (2012).

23. Ruby, J. G. *et al.* Large-scale sequencing reveals 21U-RNAs and additional microRNAs and endogenous siRNAs in C. elegans. *Cell* **127**, 1193–207 (2006).

24. Gu, W. *et al.* CapSeq and CIP-TAP identify Pol II start sites and reveal capped small RNAs as C. elegans piRNA precursors. *Cell* **151**, 1488–500 (2012).

25. Blumenthal, T. Trans-splicing and operons in C. elegans. *WormBook* 1–11 (2012) doi:10.1895/wormbook.1.5.2.

26. Weick, E.-M. *et al.* PRDE-1 is a nuclear factor essential for the biogenesis of Ruby motif-dependent piRNAs in C. elegans. *Genes Dev* **28**, 783–96 (2014).

27. Weng, C. *et al.* The USTC co-opts an ancient machinery to drive piRNA transcription in C. elegans. *Genes Dev* **33**, 90–102 (2019).

28. Perez-Borrajero, C. *et al.* Structural basis of PETISCO complex assembly during piRNA biogenesis in C. elegans. *Genes Dev* **35**, 1304–1323 (2021).

29. Wang, X. *et al.* Molecular basis for PICS-mediated piRNA biogenesis and cell division. *Nat Commun* **12**, (2021).

30. Zeng, C. *et al.* Functional Proteomics Identifies a PICS Complex Required for piRNA Maturation and Chromosome Segregation. *Cell Rep* **27**, 3561-3572.e3 (2019).

31. Goh, W.-S. S. *et al.* A genome-wide RNAi screen identifies factors required for distinct stages of C. elegans piRNA biogenesis. *Genes Dev* **28**, 797–807 (2014).

32. Zimmermann, L. *et al.* A Completely Reimplemented MPI Bioinformatics Toolkit with a New HHpred Server at its Core. *J Mol Biol* **430**, 2237–2243 (2018).

33. Jumper, J. *et al.* Highly accurate protein structure prediction with AlphaFold. *Nature* **596**, 583–589 (2021).

34. Yang, J.-Y. *et al.* Structure of Schlafen13 reveals a new class of tRNA/rRNA- targeting RNase engaged in translational control. *Nat Commun* **9**, 1165 (2018).

35. Metzner, F. J., Huber, E., Hopfner, K.-P. & Lammens, K. Structural and biochemical characterization of human Schlafen 5. *Nucleic Acids Res* **50**, 1147–1161 (2022).

36. Garvie, C. W. *et al.* Structure of PDE3A-SLFN12 complex reveals requirements for activation of SLFN12 RNase. *Nat Commun* **12**, (2021).

37. Varadi, M. *et al.* AlphaFold Protein Structure Database: massively expanding the structural coverage of protein-sequence space with high-accuracy models. *Nucleic Acids Res* **50**, D439–D444 (2022).

38. Watanabe, T. *et al.* MITOPLD is a mitochondrial protein essential for nuage formation and piRNA biogenesis in the mouse germline. *Dev Cell* **20**, 364–75 (2011).

39. Huang, H. *et al.* piRNA-associated germline nuage formation and spermatogenesis require MitoPLD profusogenic mitochondrial-surface lipid signaling. *Dev Cell* **20**, 376–87 (2011).

40. Evans, R. *et al.* Protein complex prediction with AlphaFold-Multimer. *bioRxiv* 2021.10.04.463034 (2022) doi:10.1101/2021.10.04.463034.

41. Metzner, F. J. *et al.* Mechanistic understanding of human SLFN11. *Nat Commun* **13**, 5464 (2022).

42. Yang, W. Nucleases: diversity of structure, function and mechanism. *Q Rev Biophys* **44**, 1–93 (2011).

43. de Albuquerque, B. F. M. *et al.* PID-1 is a novel factor that operates during 21U-RNA biogenesis in Caenorhabditis elegans. *Genes Dev* **28**, (2014).

44. Gan, B., Chen, S., Liu, H., Min, J. & Liu, K. Structure and function of eTudor domain containing TDRD proteins. *Crit Rev Biochem Mol Biol* **54**, 119–132 (2019).

45. Chen, C., Nott, T. J., Jin, J. & Pawson, T. Deciphering arginine methylation: Tudor tells the tale. *Nat Rev Mol Cell Biol* **12**, 629–642 (2011).

46. Bell, T. A. *et al.* The paternal gene of the DDK syndrome maps to the Schlafen gene cluster on mouse chromosome 11. *Genetics* **172**, 411–23 (2006).

47. Bartonicek, N. *et al.* The retroelement Lx9 puts a brake on the immune response to virus infection. *Nature* **608**, 757–765 (2022).

48. Li, M. *et al.* Codon-usage-based inhibition of HIV protein synthesis by human schlafen 11. *Nature* **491**, 125–8 (2012).

49. Eaglesham, J. B., McCarty, K. L. & Kranzusch, P. J. Structures of diverse poxin cGAMP nucleases reveal a widespread role for cGAS-STING evasion in host-pathogen conflict. *Elife* **9**, (2020).

50. Gubser, C. *et al.* Camelpox virus encodes a schlafen-like protein that affects orthopoxvirus virulence. *J Gen Virol* **88**, 1667–1676 (2007).

51. Glover, M. L. *et al.* NONU-1 Encodes a Conserved Endonuclease Required for mRNA Translation Surveillance. *Cell Rep* **30**, 4321-4331.e4 (2020).

52. Brenner, S. The genetics of Caenorhabditis elegans. *Genetics* **77**, 71–94 (1974).

53. Schweinsberg, P. J. & Grant, B. D. C. elegans gene transformation by microparticle bombardment. *WormBook* 1–10 (2013) doi:10.1895/WORMBOOK.1.166.1.

54. Arribere, J. A. *et al.* Efficient marker-free recovery of custom genetic modifications with CRISPR/Cas9 in Caenorhabditis elegans. *Genetics* **198**, 837–846 (2014).

55. Rappsilber, J., Mann, M. & Ishihama, Y. Protocol for micro-purification, enrichment, pre-fractionation and storage of peptides for proteomics using StageTips. *Nature Protocols 2007 2:8* **2**, 1896–1906 (2007).

56. Cox, J. & Mann, M. Quantitative, High-Resolution Proteomics for Data-Driven Systems Biology. *https://doi.org/10.1146/annurev-biochem-061308-093216* **80**, 273–299 (2011).

57. Cox, J. & Mann, M. MaxQuant enables high peptide identification rates, individualized p.p.b.-range mass accuracies and proteome-wide protein quantification. *Nature Biotechnology 2008 26:12* **26**, 1367–1372 (2008).

58. Gorrec, F. The MORPHEUS protein crystallization screen. *J Appl Crystallogr* **42**, 1035–1042 (2009).

59. Newman, J. *et al.* Towards rationalization of crystallization screening for small- to medium-sized academic laboratories: the PACT/JCSG+ strategy. *Acta Crystallogr D Biol Crystallogr* **61**, 1426–31 (2005).

60. Vonrhein, C. *et al.* Data processing and analysis with the autoPROC toolbox. *Acta Crystallogr D Biol Crystallogr* **67**, 293–302 (2011).

61. Kabsch, W. XDS. *Acta Crystallogr D Biol Crystallogr* **66**, 125–32 (2010).

62. Evans, P. R. & Murshudov, G. N. How good are my data and what is the resolution? *Acta Crystallogr D Biol Crystallogr* **69**, 1204–14 (2013).

63. McCoy, A. J. *et al.* Phaser crystallographic software. *J Appl Crystallogr* **40**, 658–674 (2007).

64. Liebschner, D. *et al.* Macromolecular structure determination using X-rays, neutrons and electrons: recent developments in Phenix. *Acta Crystallogr D Struct Biol* **75**, 861–877 (2019).

65. Cowtan, K. The Buccaneer software for automated model building. 1. Tracing protein chains. *Acta Crystallogr D Biol Crystallogr* **62**, 1002–11 (2006).

66. Emsley, P., Lohkamp, B., Scott, W. G. & Cowtan, K. Features and development of Coot. *Acta Crystallogr D Biol Crystallogr* **66**, 486–501 (2010).

67. Afonine, P. v *et al.* Towards automated crystallographic structure refinement with phenix.refine. *Acta Crystallogr D Biol Crystallogr* **68**, 352–67 (2012).

68. Williams, C. J. *et al.* MolProbity: More and better reference data for improved all-atom structure validation. *Protein Sci* **27**, 293–315 (2018).

69. Joosten, R. P., Joosten, K., Murshudov, G. N. & Perrakis, A. PDB_REDO: constructive validation, more than just looking for errors. *Acta Crystallogr D Biol Crystallogr* **68**, 484–96 (2012).

70. Pettersen, E. F. *et al.* UCSF ChimeraX: Structure visualization for researchers, educators, and developers. *Protein Sci* **30**, 70–82 (2021).

71. Mirdita, M. *et al.* ColabFold: making protein folding accessible to all. *Nat Methods* **19**, 679–682 (2022).

72. Perez-Riverol, Y. *et al.* The PRIDE database resources in 2022: a hub for mass spectrometry-based proteomics evidences. *Nucleic Acids Res* **50**, D543–D552 (2022).
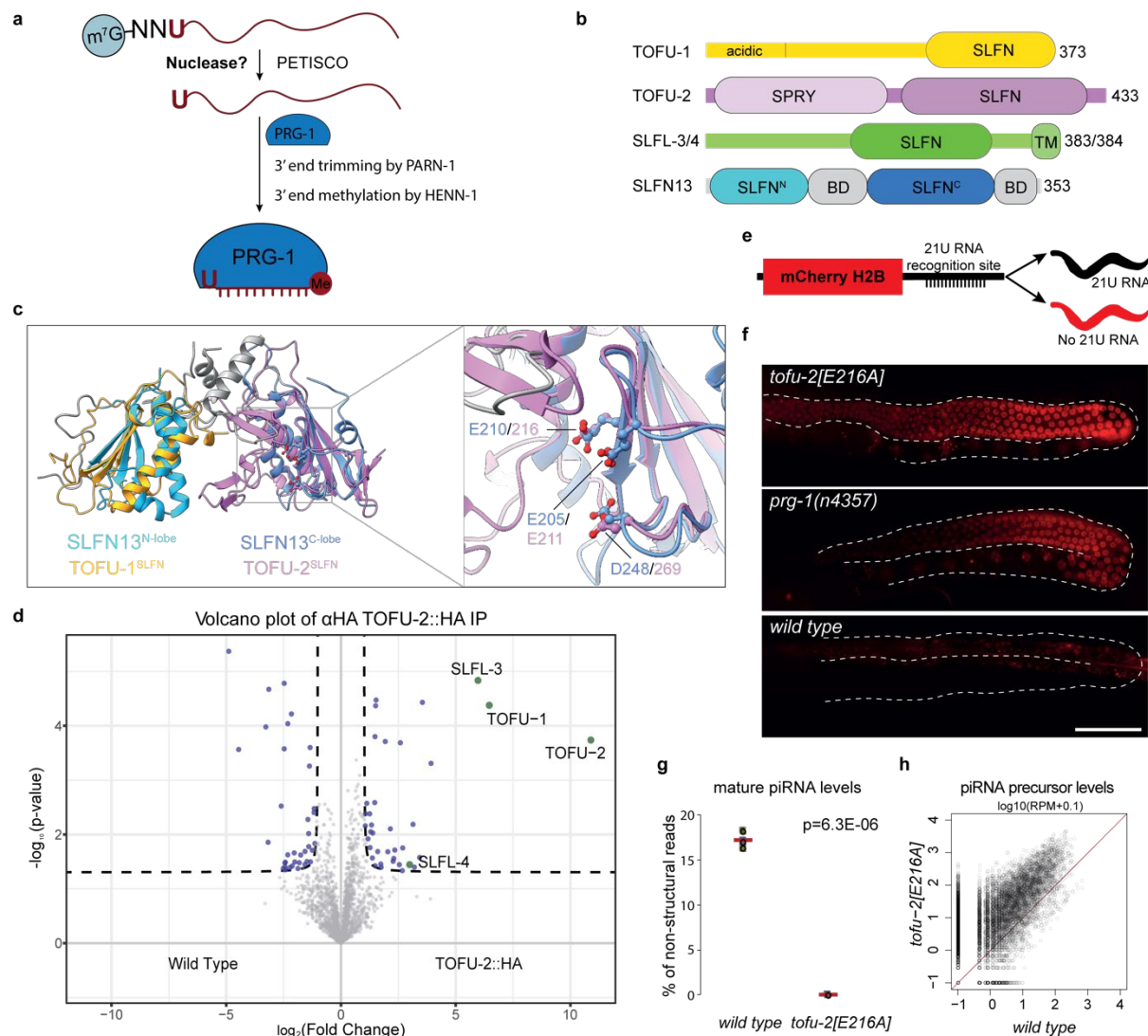
**Fig. 1 | Identification of the catalytic center of TOFU-2.**

**a**, Model of piRNA (21U RNA) formation in *C. elegans*. Individually transcribed piRNA precursors of ~27-29 nucleotides in length are stabilized by the PETISCO complex. Following removal of the 5' Cap and two nucleotides, the intermediates are loaded onto PRG-1, followed by trimming and methylation of the 3'-end by PARN-1 and HENN-1, respectively. The nuclease that is responsible for 5'-end maturation of piRNAs has remained unknown thus far.

**b**, Schematic domain organization of TOFU-1, TOFU-2 and SLFL-3/4. Lines indicate low-complexity regions and rounded rectangles indicate predicted folded domains. BD: bridging domain, TM: transmembrane domain.

**c**, Superposition of the TOFU-1 and TOFU-2 SLFN domains onto the crystal structure of the N-terminal SLFN13 endoribonuclease domain. The domains are colored as in panel (b). The SLFN domains of TOFU-1 is shown in yellow, of TOFU-2 in purple and of SLFN13 in light and dark blue. The SLFN13 bridging domains in grey. The zoom-in view shows the active site of SLFN13 and involved residues are shown as sticks.

**d**, Volcano plot representing label-free proteomic quantification of TOFU-2::HA (n=4) and wild type (n=4, WT) immunoprecipitations from young adult extracts. The X-axis represents the median fold enrichment of individual proteins in wild type (WT) versus the TOFU-2::HA

mutant strain. The Y-axis indicates −log10(P-value) calculated using Welch t-test . Dashed lines represent enrichment thresholds at p-value = 0.05 and fold change > 2, c = 0.05. Each dot represents an enriched (blue/green) or quantified (grey) proteins.

**e**, Schematic representation of the mCherry::H2B piRNA sensor. In presence of piRNAs, mCherry will be repressed, whereas in the absence of piRNA mCherry reporter will be expressed resulting in red fluorescent nuclei in the germline.

**f**, Widefield fluorescent microscopy of adult hermaphrodites carrying the piRNA sensor in three genetic backgrounds: *tofu-2[E216A]* on top, *prg-1(n4357)* in the middle, wild type at the bottom. The germlines are outlined by a white dashed line. Scale bar – 50 μm.

**g**, Total piRNA levels in wild type and *tofu-2[E216A]*-mutant young adult hermaphrodites (n = 3). Red lines depict group means and P-values were calculated using two-tailed unpaired t-test.

**h**, Scatter plot depicting the relative abundance of piRNA precursors from individual loci in *tofu-2[E216A]*-mutant versus wild type young adult hermaphrodites. RPM: Reads per million non-structural sRNA reads.
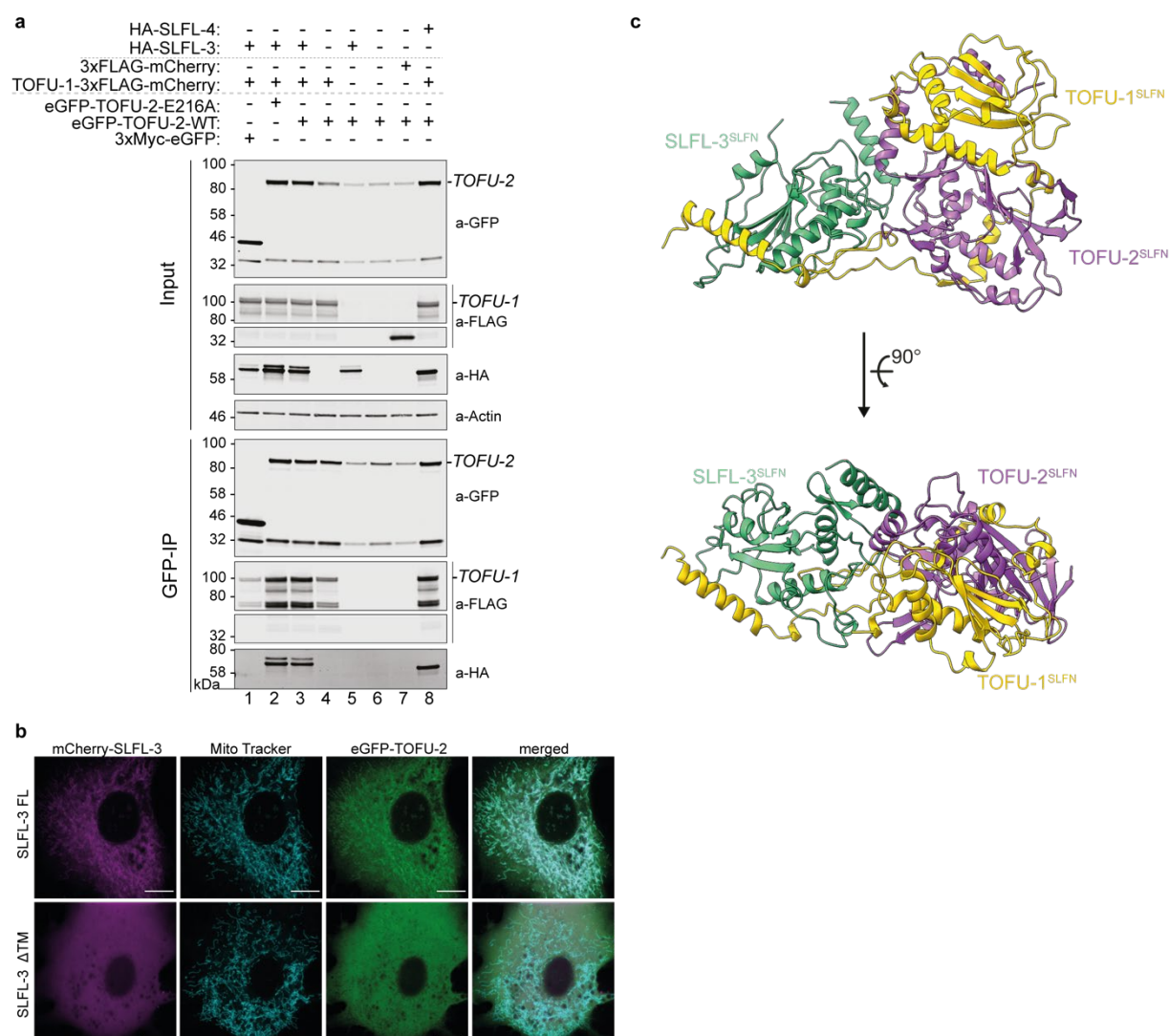
**Fig. 2 | TOFU-1, TOFU-2 and SLFL-3/4 form a mitochondria-bound complex.**

**a**, Anti-GFP immunoprecipitation from BmN4 cell lysates made from cells that were transfected with the indicated constructs. eGFP-TOFU-2 was immunoprecipitated, followed by Western blot detection of TOFU-1 (FLAG), SLFL-3 (HA) or SLFL-4 (HA). Expression of 3xMyc-eGFP and of 3xFLAG-mCherry served as negative controls.

**b**, Single-plane confocal micrographs of BmN4 cells transfected with eGFP-TOFU-2 and full-length mCherry-SLFL-3 (top) or mCherry-SLFL-3 ΔTM (bottom). TOFU-1 was also transfected but was not tagged with a fluorescent protein. Mitochondria were stained with Mito Tracker. Scale bars – 10 μm.

**c**, AlphaFold predicted structure of a minimal trimeric TOFU-1, TOFU-2, SLFL-3 complex. The best of five predicted models is shown as cartoon in two different orientations. TOFU-1 is shown in yellow, TOFU-2 in purple and SLFL-3 in green.

26

**a**

$m^7G-rArA \mid rUrUrCrCrArCrUrGrUrUrUrArGrUrUrUrGrUrCrUrGrUrUrUrArA-p*Cp$
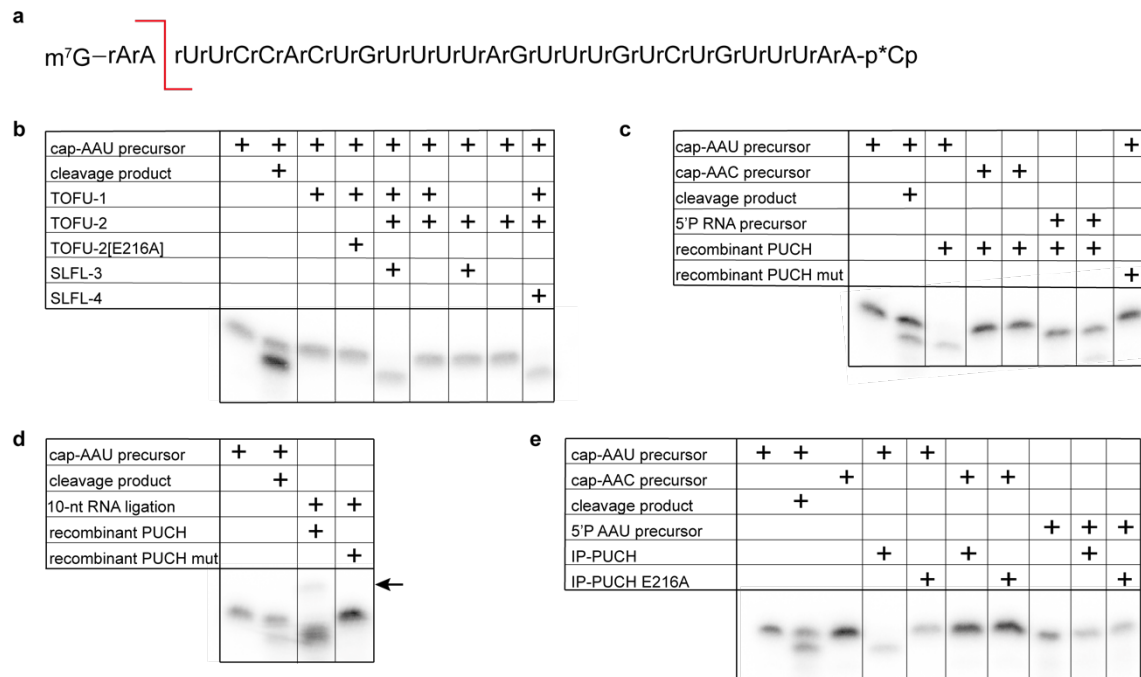
**Fig. 3 | PUCH is a Cap- and sequence-specific endoribonuclease.**

**a**, Sequence of the synthetic piRNA precursor used in the assay. Red line indicates the expected cleavage position. Both precursor and expected cleavage product were run in the two left-most lanes of every gel to mark where these molecules are to be expected.

**b**, *In vitro* cleavage assay of the piRNA precursor using GFP-IP material from BmN4 cell extracts. Cells were transfected with eGFP-TOFU-2, TOFU-1, SLFL-3 or SLFL-4 in various combinations, as indicated.

**c**, Cleavage assays with recombinant PUCH and different RNA substrates. 'Recombinant PUCH Mut' reflects a complex in which TOFU-2 was mutated in the catalytic site (TOFU-2[E216A]).

**d**, RNA obtained from a cleavage reaction (using either wild-type or TOFU-2[E216A] mutant PUCH complex) was ligated to a 10 nucleotide long 5'OH-containing RNA adapter. The ligation product is indicated with an arrow.

**e**, *In vitro* cleavage assay on different types of RNA substrate using the PUCH complex retrieved from BmN4 cells by immunoprecipitation.
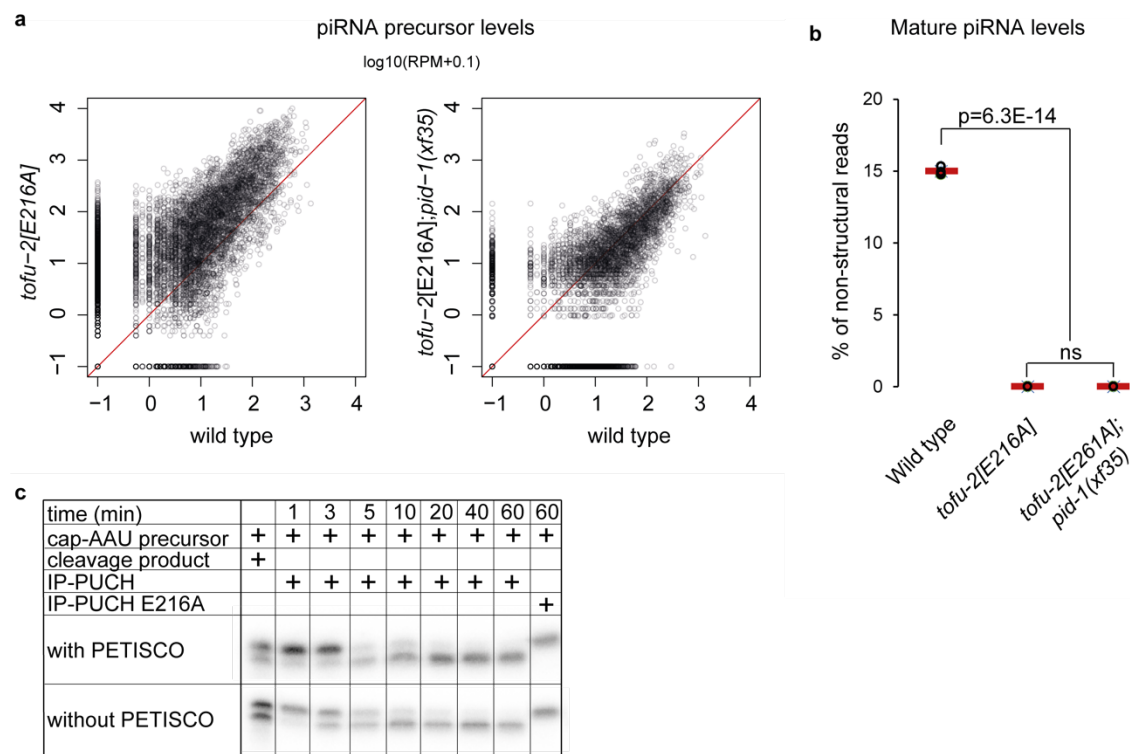
**a** piRNA precursor levels
log10(RPM+0.1)

**b** Mature piRNA levels

**c**

| time (min) | | 1 | 3 | 5 | 10 | 20 | 40 | 60 | 60 |
|---|---|---|---|---|---|---|---|---|---|
| cap-AAU precursor | + | + | + | + | + | + | + | + | + |
| cleavage product | + | | | | | | | | |
| IP-PUCH | | + | + | + | + | + | + | + | |
| IP-PUCH E216A | | | | | | | | | + |
| with PETISCO | | | | | | | | | |
| without PETISCO | | | | | | | | | |

**Fig. 4 | PETISCO is necessary for piRNA precursor accumulation *in vivo* and does not interfere with PUCH-mediated precursor cleavage.**

**a**, Scatter plots depicting the relative abundance of individual piRNA precursors in *tofu-2[E216A]*-mutant (left) and *tofu-2[E216A];pid-1(xf35)*-double mutant (right) versus wild type young adult hermaphrodites. RPM: Reads per million non-structural sRNA reads.

**b,** Total piRNA levels in wild type, *tofu-2[E216A]*-mutant and *tofu-2[E216A];pid-1(xf35)*-double mutant young adult hermaphrodites (n=3). Red lines depict group means and P-values were calculated using ANOVA test followed by Tukey HSD.

**c**, *In vitro* piRNA precursor cleavage assay either in presence or absence of the PETISCO complex in a time-series. PUCH in this experiment was isolated from BmN4 cell extracts using immune-precipitations.

28
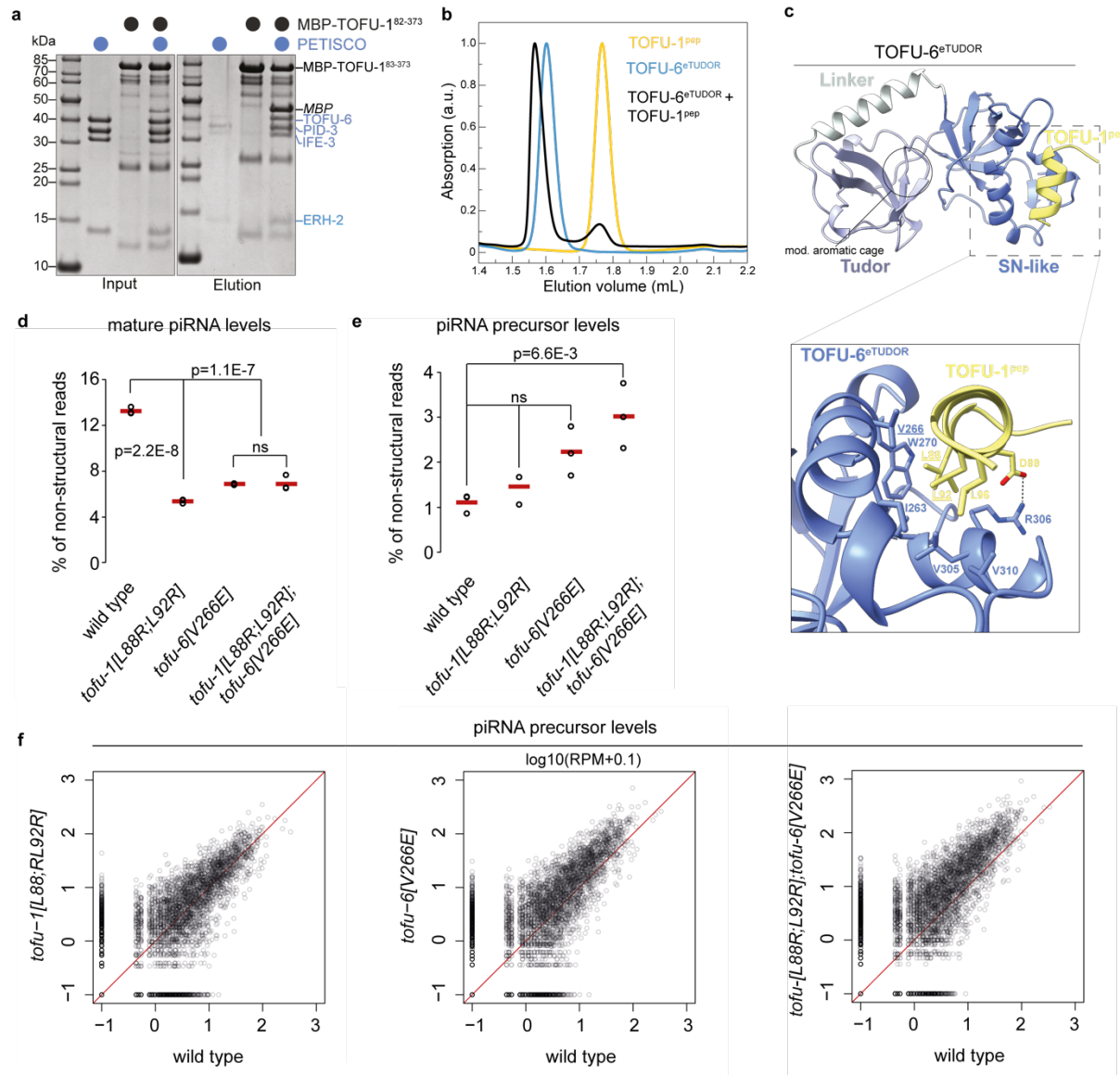
**Fig. 5 | TOFU-6 from PETISCO interacts with PUCH via TOFU-1.**

**a**, Analysis of the interaction between TOFU-1 and PETISCO by amylose pull-down assays. Purified MBP-tagged TOFU-1$^{82\text{-}373}$ was incubated with excess PETISCO. Input and elution fractions were analyzed by SDS-PAGE followed by Coomassie staining.

**b**, Purified TOFU-6$^{eTUDOR}$, TOFU-1$^{82\text{-}113}$ (=TOFU-1$^{pep}$) and a mixture thereof were subjected to size exclusion chromatography. Chromatograms: TOFU-6$^{eTUDOR}$ (blue), TOFU-1$^{pep}$ (yellow) and TOFU-6$^{eTUDOR}$ + TOFU-1$^{pep}$ (black).

**c**, Crystal structure of the TOFU-6$^{eTUDOR}$–TOFU-1$^{pep}$ complex shown as cartoon. The TOFU-6$^{eTUDOR}$ domain is shown in different shades of blue and TOFU-1$^{pep}$ in yellow. The zoom-in view shows the interaction interface; involved residues are shown as sticks.

**d and e**, Total mature (**d**) and precursor (**e**) piRNA levels in wild-type, *tofu-1[L88R;L92R], tofu-6[V266E]* and *tofu-1[L88R;L92R];tofu-6[V266E]*-double mutant young adult hermaphrodites (n = 3). Red lines depict group means and P-values were calculated using ANOVA test followed by Tukey HSD.

**f**, Scatter plots depicting the relative abundance of precursors from individual piRNA loci in *tofu-1[L88R;L92R]* (left)*, tofu-6[V266E]* (middle) and *tofu-1[L88R;L92R];tofu-6[V266E]*-double

1    mutant (right) versus wild-type young adult hermaphrodites. RPM: Reads per million non-
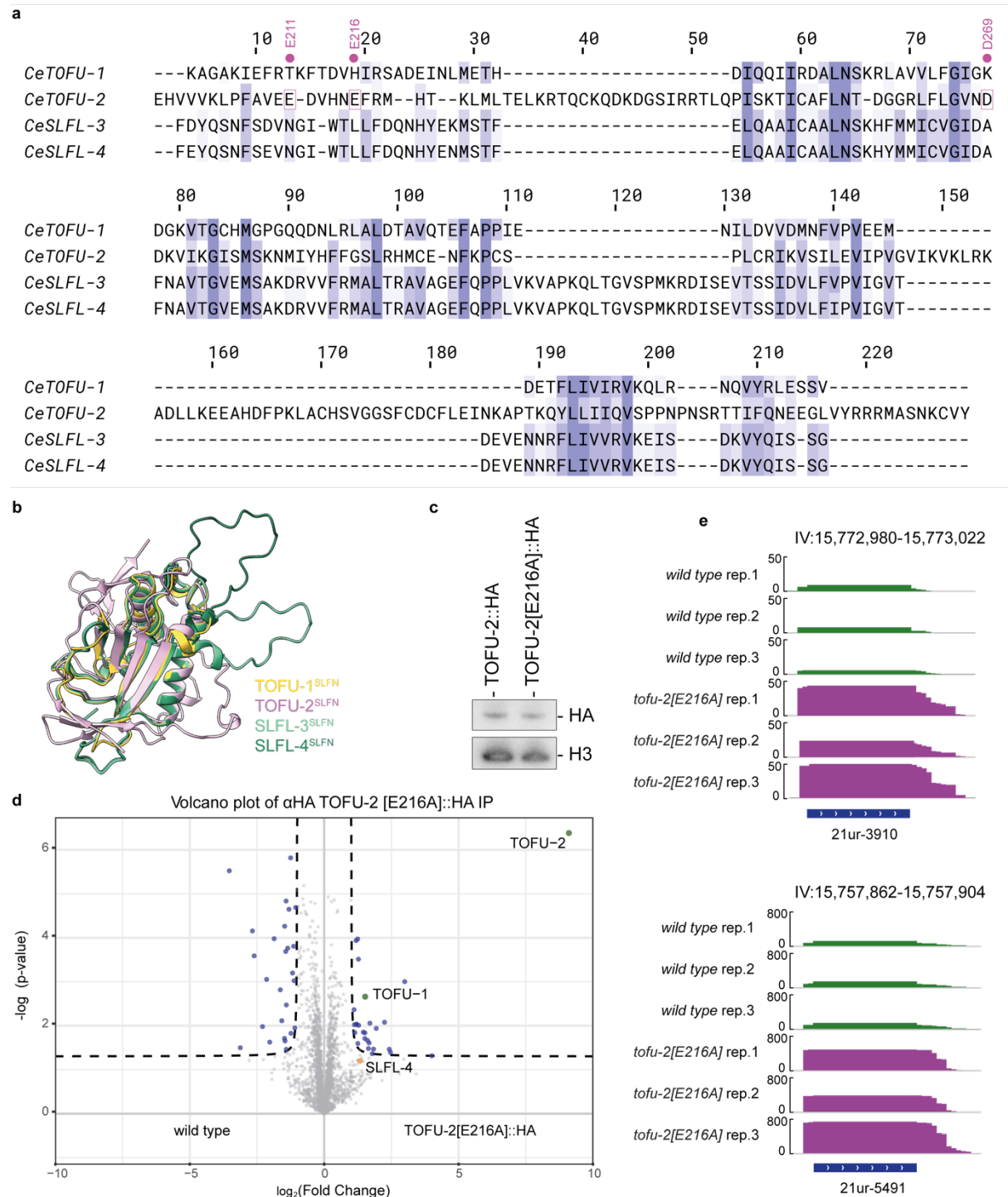2    structural sRNA reads. The underlying data is the same as in panel **e**.

**Fig. S1 | Mutation in the catalytic center of TOFU-2 does not affect protein stability and interaction with TOFU-1.**

**a**, Structure-based sequence alignment of the SLFN domains from TOFU-1, TOFU-2, SLFL-3 and SLFL-4. The acidic residues from the active site of TOFU-2 are highlighted with purple boxes and the residue number is indicated on the top.

**b**, Superposition of the AlphaFold predicted SLFN domains fromTOFU-1, TOFU-2, SLFL-3 and SLFL-4. TOFU-1 is shown in yellow, TOFU-2 in purple and the paralogs SLFL-3/4 in different shades of green.

31

1    **c**, Extracts of young adult worms with genotype *tofu-2::HA* and *tofu-2[E216A]::HA*, were

2    separated on SDS-PAGE. Western blot was probed using anti-HA and anti-H3 antibodies,

3    followed by visualization with HRP.

4    **d,** Volcano plot representing label-free proteomic quantification of TOFU-2[E216A]::HA (n=4)

5    and wild type (n=4, WT) immunoprecipitations from young adult extracts. The X-axis

6    represents the median fold enrichment of individual proteins in wild type (WT) versus the

7    TOFU-2::HA mutant strain. The Y-axis indicates $-\log_{10}$(P-value) calculated using Welch t-test.

8    Dashed lines represent enrichment thresholds at p-value = 0.05 and fold change > 2, c = 0.05.

9    Each dot represents an enriched (blue/grey) or quantified (orange) proteins.

10   **e,** Genome browser tracks of two individual piRNA loci, displaying normalized read coverage

11   in piRNA precursor libraries. Top three tracks (green) are from a wild-type background, the

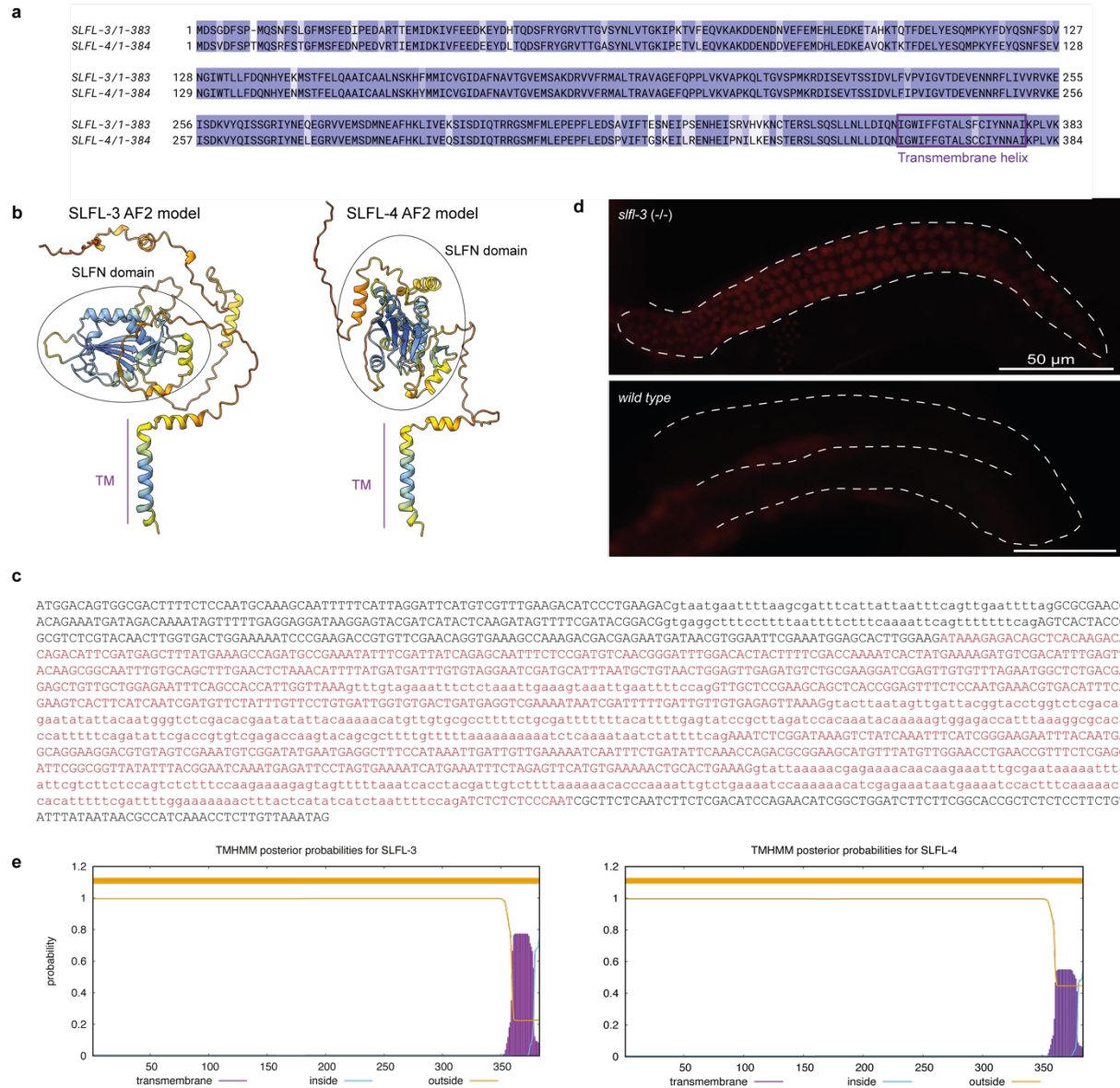12   bottom three tracks (purple) are from a *tofu-2[E216A]* mutant background.

**Fig. S2 | SLFL-3 and SLFL-4 are transmembrane proteins involved in piRNA biogenesis in *C. elegans*.**

**a**, Sequence alignment of SLFL-3 and SLFL-4. The predicted C-terminal transmembrane helix is highlighted with a box.

**b**, AlphaFold2 predicted structures of SLFL-3/4 shown as cartoon and colored by pLDDT score, which reports on the model confidence. Dark blue indicates very high, light blue confident, yellow low and orange very low model confidence.

**c**, Sequence of *slfl-3(xf248)* allele. Deleted sequence is marked in red.

**d**, Widefield fluorescent microscopy of adult hermaphrodites carrying the mCherry::H2B-piRNA sensor in two genetic backgrounds: *slfl-3(xf248)* on top and wild type at the bottom. The germlines are outlined by a white dashed line. Scale bar – 50 μm.

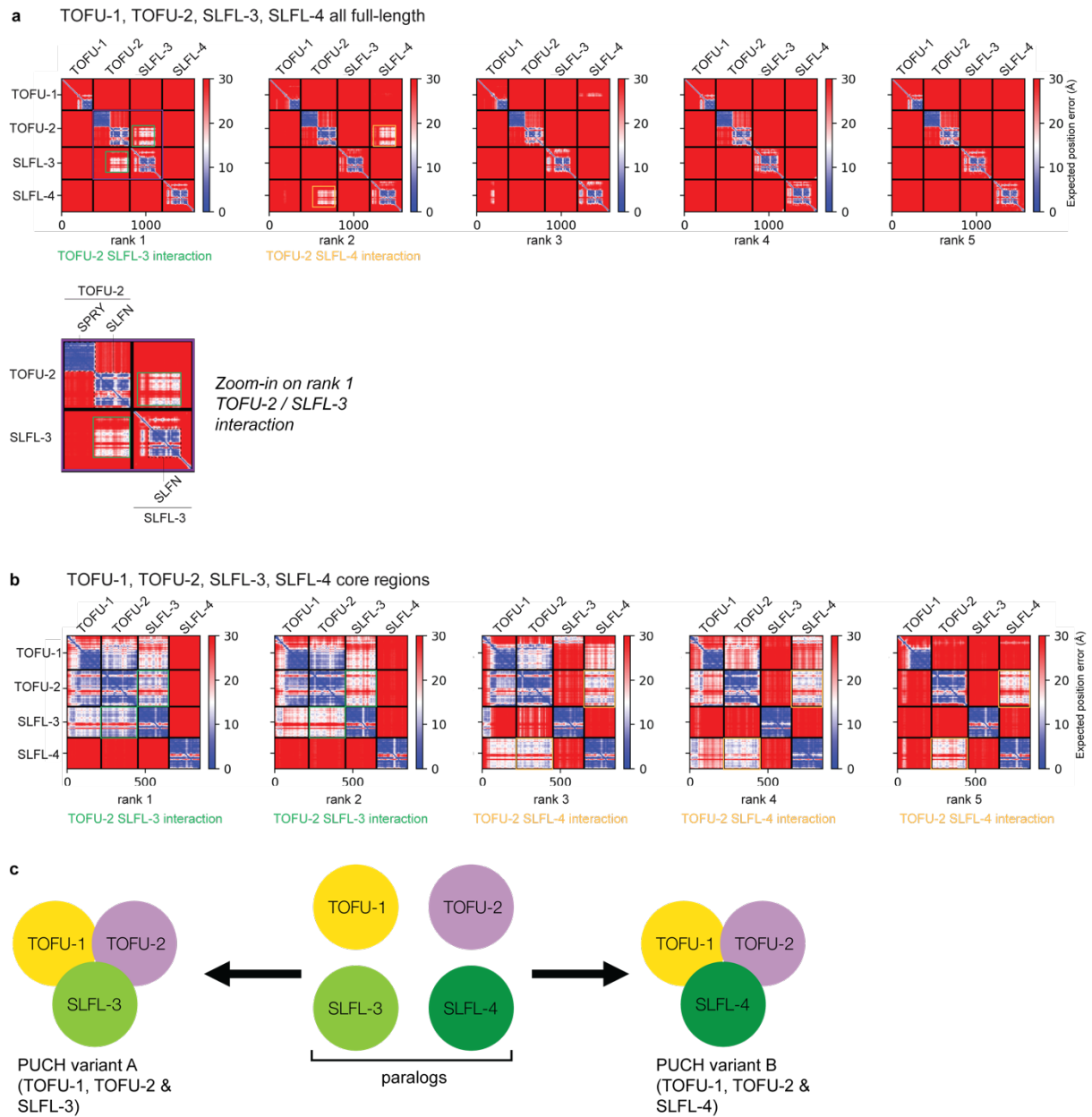**e**, Prediction of transmembrane helices in SLFL-3 and SLFL-4 using TMHMM - 2.0.

**Fig. S3 | AlphaFold predicts a trimeric complex consisting of TOFU-1, TOFU-2 and either SLFL-3 or SLFL-4.**
**a**, Predicted alignment error (PAE) plots for the five models predicted by Alphafold for full-length TOFU-1, TOFU-2, SLFL-3 and SLFL-4. The zoom-in highlights the predicted interaction between the SLFN domains of TOFU-2 and SLFL-3, suggesting that the TOFU-2 SPRY domain is no involved in complex formation. The expected position error in angstroms (Å) is color coded where blue color indicates low PAE (high confidence) and red color indicates high PAE (low confidence).
**b**, Predicted alignment error (PAE) plots for the five models predicted by Alphafold for core regions of TOFU-1, TOFU-1, SLFL-3 and SLFL-4.
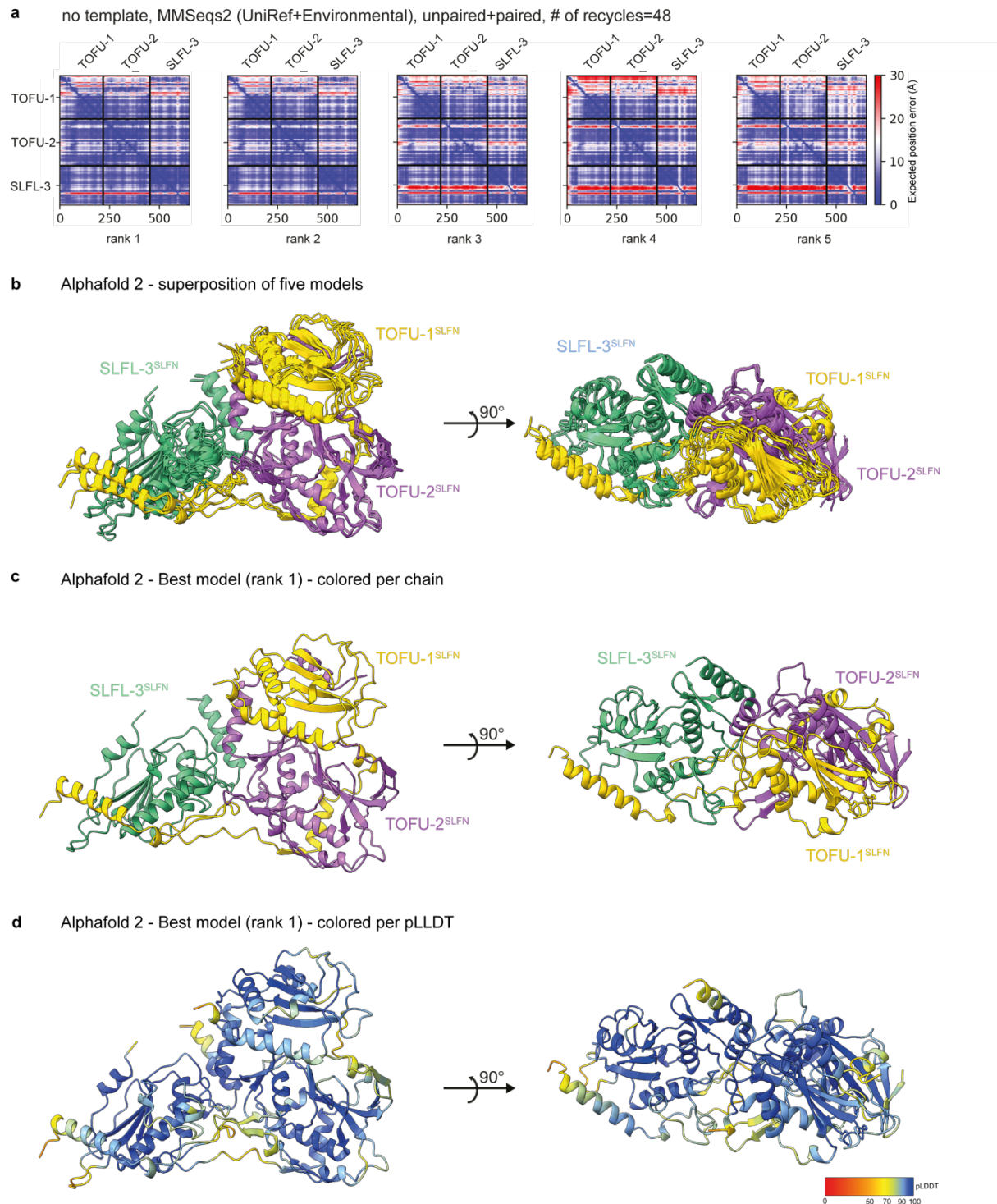**c**, Schematic summary of the interaction results presented in panels **a** and **b**

34

**a** no template, MMSeqs2 (UniRef+Environmental), unpaired+paired, # of recycles=48

**b** Alphafold 2 - superposition of five models

**c** Alphafold 2 - Best model (rank 1) - colored per chain

**d** Alphafold 2 - Best model (rank 1) - colored per pLLDT

1
2
3 **Fig. S4 | AlphaFold structure prediction of the trimeric complex consisting of TOFU-1, TOFU-**
4 **2 and SLFL-3 shows convergence of models.**
5 **a**-**b**, AlphaFold predicts a trimeric complex consisting of TOFU-1, TOFU-2 and SLFL-3. TOFU-1
6 residues 156-373, TOFU-2 residues 200-433 and SLFL-3 residues 103-300 were used for the
7 prediction. The predicted alignment error (PAE) plots are shown in (a), the five superposed
8 models are shown as cartoon in (b). TOFU-1 is colored yellow, TOFU-2 purple and SLFL-3
9 green. The settings used for the prediction are shown on the top. The expected position error

35

1  in angstroms (Å) is color coded where blue color indicates low PAE (high confidence) and red
2  color indicates high PAE (low confidence).
3  **c-d**, The best of the five predicted models is colored per chain (**c**) or per pLDDT score (**d**),
4  which reports on the model confidence. Dark blue indicates very high, light blue confident,
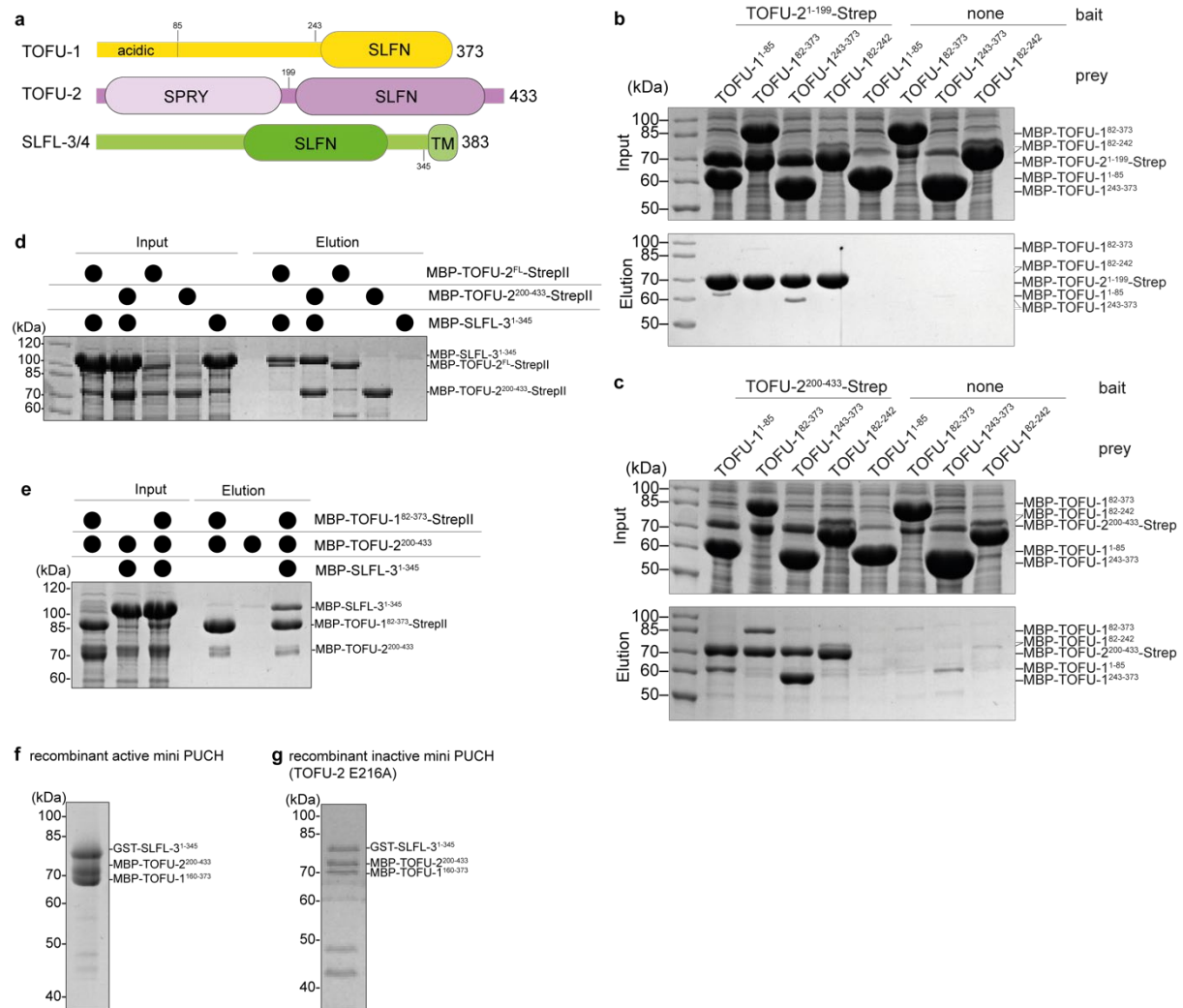5  yellow low and orange very low model confidence.

**Fig. S5 | Verification of SLFL-interactions obtained by AlphaFold using recombinant proteins.**

**a**, Schematic domain organization of TOFU-1, TOFU-2 and SLFL-3. Lines indicate low-complexity regions and rounded rectangles indicate predicted folded domains. TM: transmembrane domain.

**b-c**, A construct containing the TOFU-1 SLFN domain binds to the TOFU-2 SLFN domain while the TOFU-2 SPRY domain does not bind TOFU-1. Analysis of the interaction of different TOFU-1 constructs with the StrepII-tagged TOFU-2 SPRY domain in (b) and StrepII-tagged TOFU-2 SLFN domain in (c). The indicated constructs were co-expressed in *E. coli* and the StrepII-tagged bait was precipitated by Streptactin XT beads. Input and elution fractions were analyzed by SDS-PAGE followed by Coomassie staining.

**d**, SLFL-3 interacts with the TOFU-2 SLFN domain. Analysis of the interaction of different StrepII-tagged TOFU-2 constructs with the SLFL-3. The indicated constructs were co-expressed in *E. coli* and the StrepII-tagged bait was precipitated by Streptactin XT beads. Input and elution fractions were analyzed by SDS-PAGE followed by Coomassie staining.

**e**, TOFU-1, TOFU-2 and SLFL-3 form a trimeric complex. Different combinations of StrepII-tagged TOFU-1, TOFU-2 and SLFL-3 were co-expressed in *E. coli* and the StrepII-tagged bait was precipitated by Streptactin XT beads. Input and elution fractions were analyzed by SDS-PAGE followed by Coomassie staining.

1  **f** and **g**, Recombinant, purified mini PUCH from *E. coli* in the active form (**f**) and inactive form
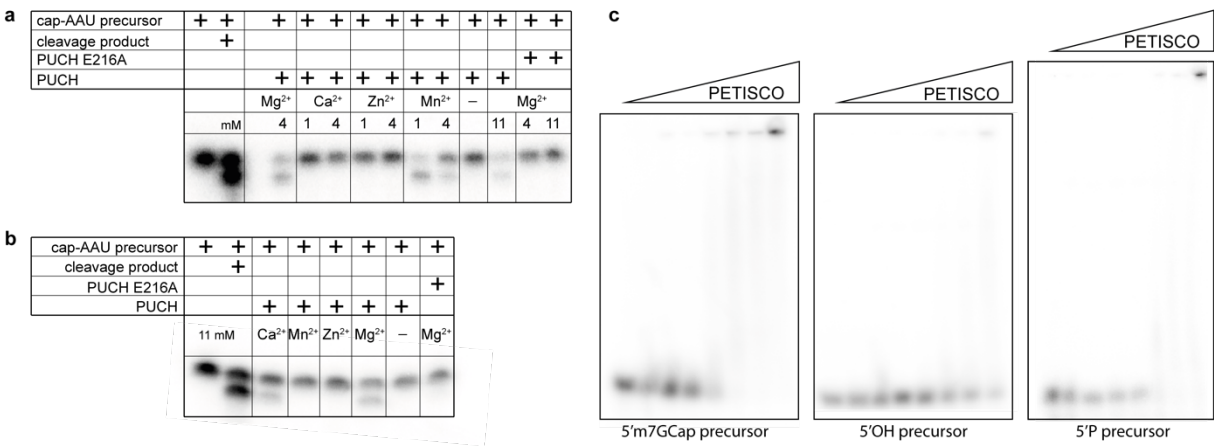
2  TOFU-2 E216A (**g**).

**Fig. S6 | Divalent cation dependence of PUCH and RNA binding by PETISCO.**

**a-b**, Cleavage assays using GFP-IP material from BmN4 cell extracts and different divalent cations in various concentrations.

**c**, Electrophoretic mobility shift assay between PETISCO complex and piRNA precursor with various 5'-ends.
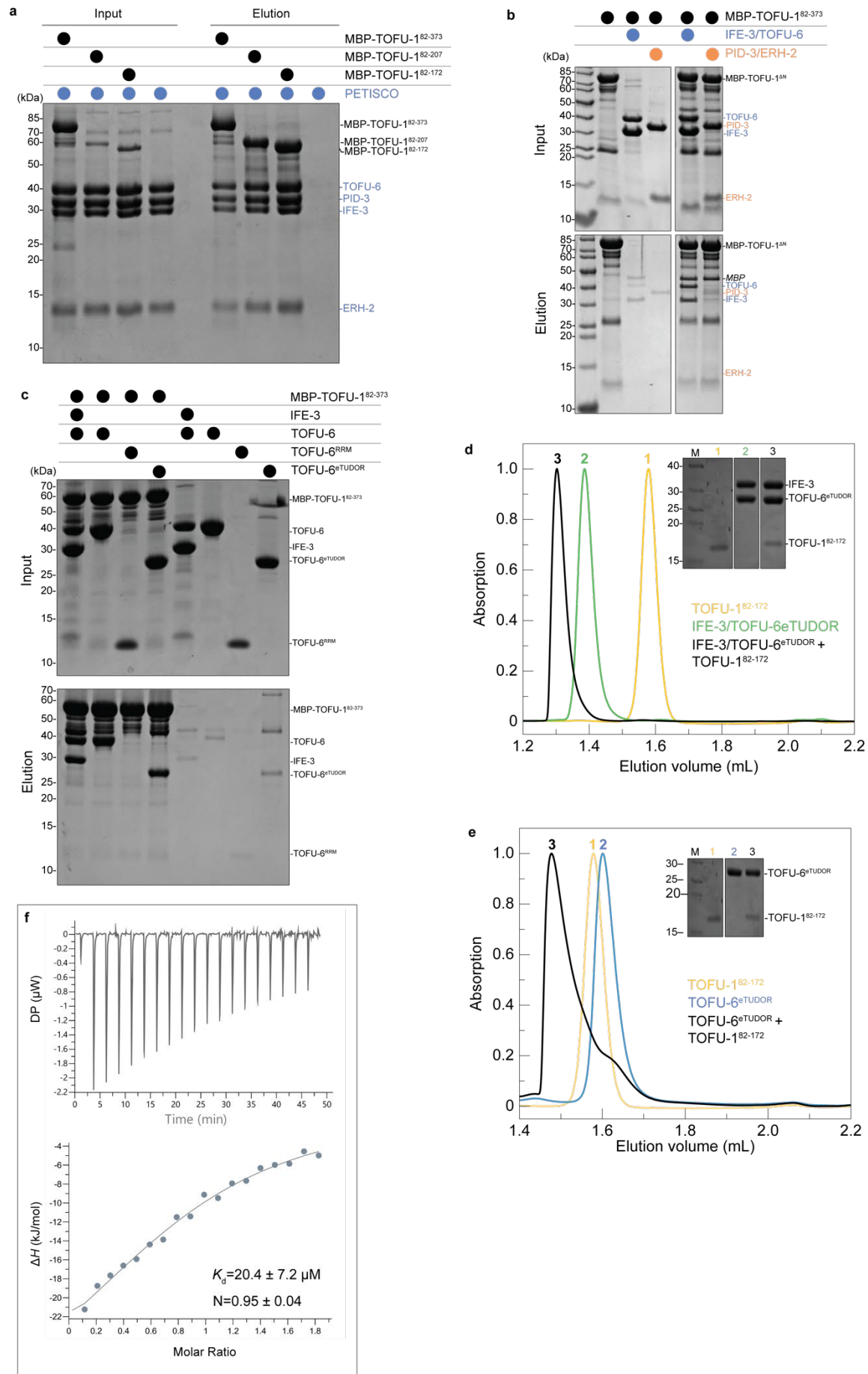
1

**Fig. S7 | A peptide upstream of the TOFU-1 SLFN domain binds to the TOFU-6 eTUDOR domain.**

**a-c**, Analysis of the interaction of different TOFU-1 constructs with PETISCO and its subunits by amylose pull-down assays. Input and elution fractions were analyzed by SDS-PAGE followed by Coomassie staining. a, Various purified MBP-tagged TOFU-1 truncations were incubated with excess PETISCO and precipitated using amylose beads. b, Purified MBP-tagged TOFU-1$^{82-373}$ was incubated with excess of the IFE-3/TOFU-6 and PID-3/ERH-2 subcomplexes precipitated using amylose beads. c, Purified MBP-tagged TOFU-1$^{82-373}$ was incubated with excess of the IFE-3/TOFU-6 subcomplex, the TOFU-6 RRM and the TOFU-6 eTUDOR domain and precipitated using amylose beads.

**d**, Purified IFE-3/TOFU-6$^{eTUDOR}$ subcomplex, TOFU-1$^{72-182}$ and a mixture thereof were subjected to size exclusion chromatography. Chromatograms: IFE-3/TOFU-6$^{eTUDOR}$ (green), TOFU-1$^{72-182}$ (yellow) and IFE-3/TOFU-6$^{eTUDOR}$ + TOFU-1$^{72-182}$ (black). The inset shows a Coomassie-stained SDS polyacrylamide gel of the peak fractions from size exclusion chromatography.

**e,** Purified TOFU-6$^{eTUDOR}$, TOFU-1$^{82-182}$ and a mixture thereof were subjected to size exclusion chromatography. Chromatograms: TOFU-6$^{eTUDOR}$ (blue), TOFU-1$^{182}$ (yellow) and TOFU-6$^{eTUDOR}$ + TOFU-1$^{182}$ (black).The inset shows a Coomassie-stained SDS polyacrylamide gel of the peak fractions from size exclusion chromatography. Note: The chromatogram of TOFU-1$^{82-172}$ (yellow) is shown for comparison and is the same as shown in panel **d**. Also, the lanes of the polyacrylamide gel are derived from the same gel in as in panel d; thus lane 1 and the marker are identical for panels **d** and **e**.

**f**, Binding of TOFU-6$^{eTUDOR}$ to TOFU-1$^{pep}$ measured by ITC. The binding affinity ($K_d$) and the stoichiometry (N) are the mean of three experiments and displayed error is the standard deviation. The experiment shows one of the three experiments as representative example.
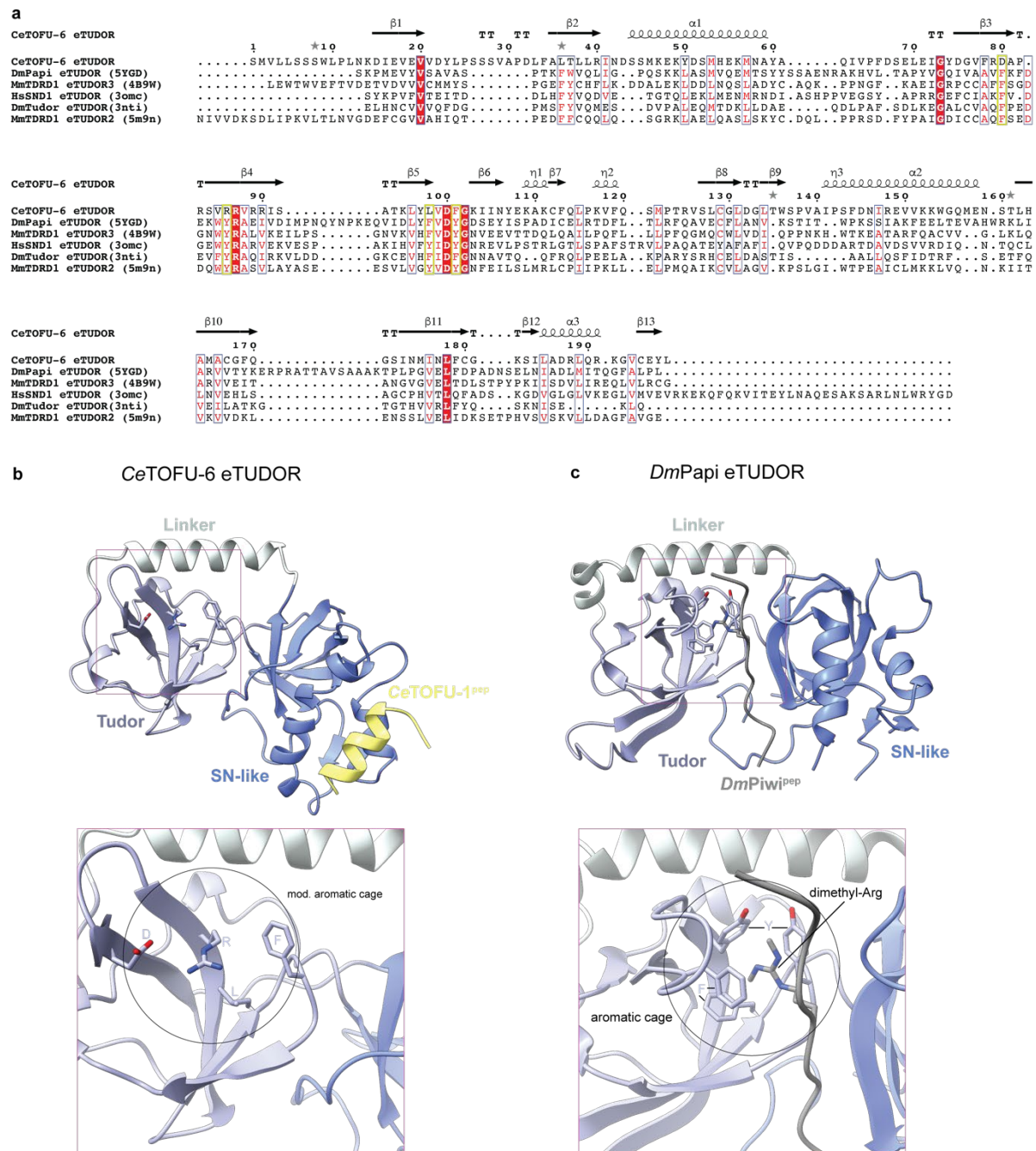
41

**Fig. S8 | Comparison of the CeTOFU-6 eTUDOR domain to canonical eTUDOR domains.**

**a**, Structure-based sequence alignment of experimentally determined eTUDOR domains. Ce, *Caenorhabditis elegans*; Dm, *Drosophila melanogaster*; Mm, *Mus musculus* and Hs, *Homo sapiens*. The PDB ID is given in brackets. The secondary structure elements are indicated above the sequence and the four residues forming the aromatic cage in canonical eTUDOR domains are highlighted by yellow boxes.

**b and c**, Crystal structures of the *C. elegans* TOFU-6^eTUDOR–TOFU-1^pep and *D. melanogaster* PAPI^eTUDOR–PIWI^pep complexes shown as cartoon. The eTUDOR domains are shown in different shades of blue, the TOFU-1^pep in yellow and the PIWI^pep containing the dimethyl-arginine residue in grey. The zoom-in view shows the region of the degenerated aromatic cage of TOFU-6^eTUDOR (**b**) and the canonical aromatic cage of PAPI^eTUDOR (**c**).
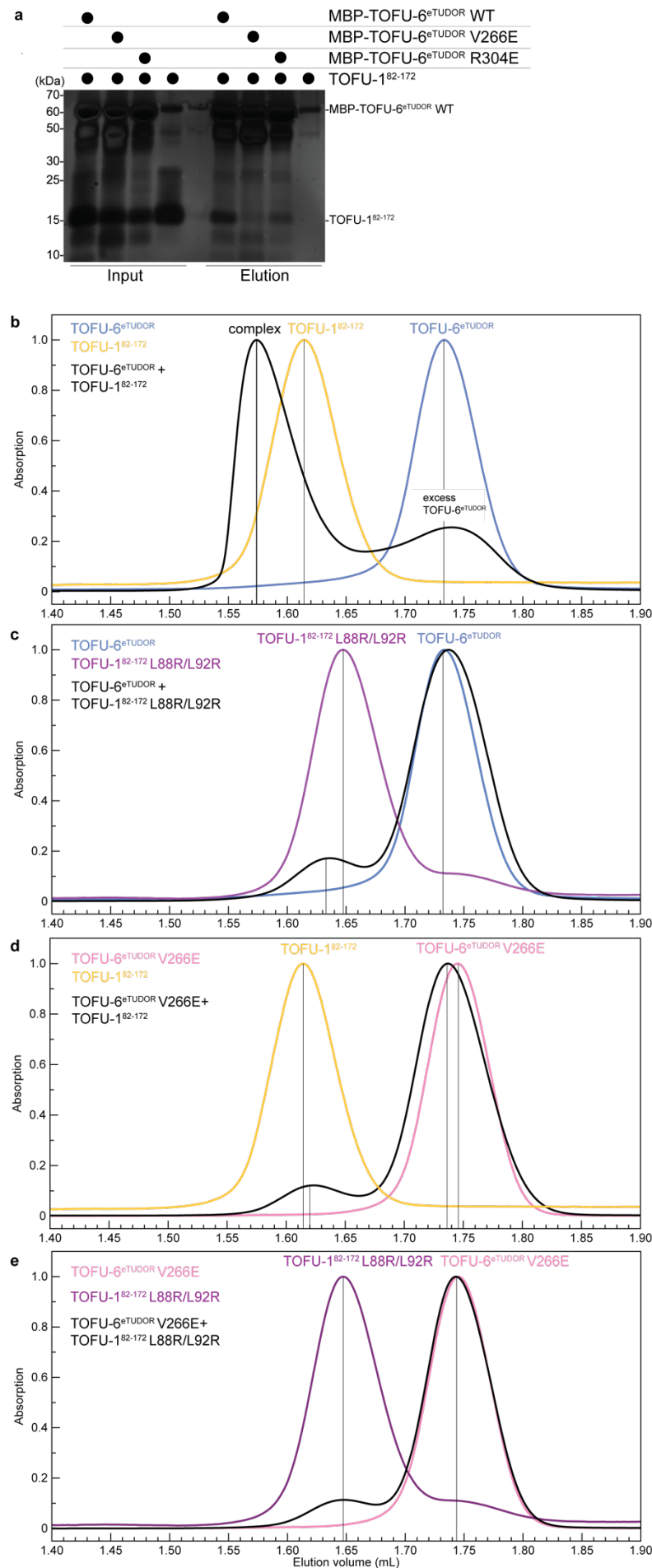
**Fig. S9 | Structure-based analysis of the TOFU-6/TOFU-1 interaction.**

**a**, Pull-down assays with purified recombinant wild-type and mutant versions of MBP-TOFU-6$^{eTUDOR}$ domain as bait and TOFU-1$^{82-172}$ as prey. Input and elution fractions were analyzed by SDS-PAGE followed by silver staining.

**b-e**, Analysis of the interaction between TOFU-1 and PETISCO by size exclusion chromatography. Purified recombinant wild-type and mutant versions of TOFU-6$^{eTUDOR}$ and TOFU-1$^{82-172}$ and mixtures thereof were subjected to size exclusion chromatography. Chromatograms: TOFU-6$^{eTUDOR}$ (blue), TOFU-1$^{82-172}$ (yellow), TOFU-6$^{eTUDOR}$ V266E (pink), TOFU-1$^{82-172}$ L88R/L92R (violet); the mixture of the respective proteins is always shown in black.